Two distinct waves of transcriptome and translatome remodelling drive germline stem cell differentiation

Tamsin J. Samuels[1,2#], Jinghua Gui[1#], Daniel Gebert[1,2], Felipe K. Teixeira[1,2,*]

[1] Department of Genetics, University of Cambridge, Downing Street CB2 3EH, Cambridge, UK

[2] Department of Physiology, Development and Neuroscience, University of Cambridge, Downing Street CB2 3DY, Cambridge, UK

#These authors contributed equally

[*]Corresponding author: fk319@cam.ac.uk

Abstract

Development and tissue maintenance require a supply of new cells, which are generated by division of stem cells and then specialised to perform their function. The differentiation process requires the tight control of gene expression, but this has been challenging to study in a systematic manner in adult stem cells, which are sparsely distributed in tissues. We have overcome these limitations by establishing a robust protocol to synchronise *Drosophila* female germline stem cell (GSC) differentiation *in vivo,* allowing us to perform transcriptome and translatome analyses at high temporal resolution during differentiation. As well as observing dynamic changes in mRNA level, promoter usage and exon inclusion, our data reveal that changing translation efficiency is the predominant regulatory mechanism during GSC differentiation. Indeed, changes in mRNA level are frequently buffered by changes in translation efficiency, including the translational repression of transcripts that will only be translated later during oocyte maturation or embryo development. Contrary to the expected linear accumulation of changes from stem cell to differentiated cell, our data reveal that differentiation occurs through two distinct waves of changes in both the transcriptome and translatome level.

Introduction

Adult stem cells divide repeatedly, replenishing the stem cell population while producing daughter cells that undergo a change in fate and differentiate to specialised cell types. The initial fate change is often driven by a master differentiation factor, which may be either asymmetrically segregated to one daughter cell, or upregulated in response to exclusion from a stem cell niche[1,2]. Many master differentiation factors have been identified by their mutant phenotypes: blocking differentiation while accumulating stem cells. However, understanding the changes downstream of the master regulator is much more complex and experimentally challenging, especially in adult stem cells such as in the hematopoietic system, gut and skin[3–6]. Adult stem cells are found in small numbers and can be quiescent for long periods, making it difficult to purify different stages of differentiation from living organisms, or to culture them *in vitro*.

Drosophila ovarian germline stem cells (GSCs) divide throughout adulthood to produce the oocytes, and are one of the best characterised *in vivo* stem cell systems[7]. GSCs are located at the anterior of the ovary in a structure called the germarium, which houses the entire differentiation process (**Figure 1A**)[8]. GSCs are maintained in a stem cell niche, receiving Dpp/BMP signalling from the somatic cap cells. With each division, one cell is retained in the stem cell niche, while the other is normally excluded from the niche and initiates differentiation. The differentiating daughter cell (cystoblast, CB) undergoes four mitotic divisions with incomplete cytokinesis, resulting in a 16 cell cyst (16cc) interconnected by a cytoplasmic bridge and a structure called the fusome. One of the 16 cells is selected to be the oocyte and meiosis is initiated, while the other 15 cells become nurse cells. Together with surrounding somatic epithelial cells, the 16cc will then form an egg chamber, beginning the process of vitellogenesis to produce the egg.

The master regulator of differentiation in GSCs is *bag-of-marbles* (*bam*)[9]. Dpp signalling from the somatic niche represses *bam* transcription in GSCs, so when a daughter cell is excluded from the niche, *bam* is transcriptionally upregulated and drives initiation of differentiation[10,11]. *bam* mutants cannot differentiate and so mutant ovaries accumulate GSC-like cells, the phenotype for which the gene is named. Indeed, most of the current understanding of GSC differentiation was brought about by the study of mutants affecting either stem cell self-renewal or differentiation[12]. In the GSC, the RNA binding complex formed by Pumilio (Pum) and Nanos (Nos) acts to repress translation of genes required for differentiation[13,14]. In the CB, Bam, together with its cofactor Benign gonial cell neoplasm (Bgcn), targets Pum and negatively regulates the Pum/Nos complex, allowing translation of the differentiation genes[15]. During the 4cc to 16cc stages, a burst of the RNA binding protein (RBP) Rbfox1 is observed in the cytoplasm[16]. Rbfox1 was shown to inhibit Pum translation, helping to consolidate the differentiation process[17]. Despite the identification of such players, many of which are RBPs, the cohorts of genes regulated by these and other uncharacterised factors during differentiation are unknown. Later during vitellogenesis, RBPs and translation regulation play another well-studied role in repressing premature production of protein from maternally deposited transcripts in the oocyte[18].

While the understanding of the regulatory mechanisms driving GSC differentiation is limited, a myriad of cellular changes occur from GSC to 16cc. The most obvious is a switch from complete cytokinesis in the GSC, which depends on ribosome biogenesis[19], to incomplete cytokinesis in differentiating cysts via decay of the ESCRT-II machinery[20–23]. Ribosome biogenesis is high in GSCs and is suppressed during differentiation[24,25]. At the same time, we have reported that global translation levels are upregulated in early differentiating cells compared to GSCs[19] and this is necessary for differentiation[26]. During differentiation, the microtubule network reorganises such that the minus ends orient to the fusome and then the future oocyte[27], leading to the oocyte accumulating markers such as *oskar* (*osk*) mRNA[28], the oo18 RNA-binding protein (Orb)[29] and mitochondria[30]. The mitochondria also undergo morphological changes, increasing the number of cristae during differentiation through the dimerisation of ATP synthase[31]. Homologous chromosomes are unpaired in GSCs and undergo pairing from the 2cc to 8cc stages such that at the end of differentiation at the 16cc stage, chromosomes are paired in time for the initiation of meiosis[32]. These examples illustrate the extent and complexity of cellular changes during GSC differentiation but the regulatory processes directing them at a gene expression level are unknown.

Available methodology has limited the study of gene expression changes and regulation during GSC differentiation, as sequencing experiments on whole ovaries do not capture the early stages of differentiation. Systematic RNA imaging has been used genome-wide to

study gene expression patterns in the ovary[33], but these scalable methods have not achieved sufficient resolution in the germarium, where stem cell differentiation occurs. Developmental staging, genetic tools and FACS purification have been used to study the transcriptome of GSCs[34,35], which have been compared to mixed differentiating cysts[36] and early follicle stages[37]. Most recently, single cell RNA sequencing has been performed on whole ovaries by several groups[38–41], identifying mRNA expression signatures of undifferentiated germline cells, immature and mature nurse cells and oocytes, as well as many different somatic cell types of the ovary. Pseudotime analysis has been used to subcluster germline cells but, due to the low depth of existing single cell technologies, present a superficial view of the changes in the transcriptome. Furthermore, the technologies to assess translation regulation at a single cell level are still in their infancy[42]. Therefore, the genome-wide assessment of the transcriptome and translatome with high temporal resolution throughout differentiation of any *in vivo* stem cell system has not been achieved, hindering our understanding of the complex changes happening downstream of master regulators.

We have leveraged established genetic tools to synchronise GSC differentiation *in vivo*[43–45]. In this system, we make use of a *bam* mutant to generate ovaries containing large pools of undifferentiated GSC-like cells. A heat shock promoter is then used to induce Bam expression and drive synchronous entry into differentiation. Ovary isolation at given time points after heat shock produces a sample enriched for GSCs or cysts at a given stage of differentiation. This protocol allows collection of sufficient material for genome-wide experiments including RNA-seq (measuring the transcriptome) and Ribo-seq (measuring the translatome) at high temporal resolution during the GSC differentiation process (6 time points from GSC to 16cc). We have extensively validated this method against *wild type* GSC differentiation using imaging-based methods. During the differentiation process from stem cell to 16cc, we find that the transcriptome undergoes a more significant transformation than anticipated, but nevertheless, the translatome undergoes 3-fold more changes than the transcriptome. Rather than a continuum of accumulating changes throughout differentiation, our data reveal two waves of global gene expression change at the level of both the transcriptome and translatome. The early wave upregulates cell cycle genes and downregulates translation-related genes, while the late wave upregulates genes involved in terminal differentiation (oogenesis and meiosis). Our data facilitate insights into the mechanisms behind this regulation during differentiation, including changes in promoter usage, splicing and translation efficiency, and will be a valuable resource for developmental biologists. These datasets provide a framework for the remodelling of the transcriptome and translatome during differentiation, revealing the existence of an unanticipated non-continuous path from stem cell to terminal differentiation.

Results

Establishing a robust protocol to synchronise GSC differentiation *in vivo*

Female *bam*$^{-/-}$ mutant flies accumulate GSC-like cells that fill their ovaries, and these samples have been used previously to examine the transcriptome and translatome of the GSC[34,46,47]. To measure gene expression changes with high developmental resolution during differentiation, we took inspiration from methods that induce germline differentiation by coupling a *bam*$^{-/-}$ mutant with a transgene that can drive differentiation through brief restoration of Bam via a heat shock promoter (*bam*$^{-/-}$*,hs-bam*)[36,44,45,48]. Previous studies in the adult ovary have found that the introduction of Bam via a heat shock promoter can drive differentiation in *bam*$^{-/-}$ mutants such that ovaries contain well-formed egg chambers after 6-8 days[43]. Therefore we asked whether shorter time points after Bam induction in a *bam*$^{-/-}$*,hs-bam* ovary could be used to collect samples enriched for different stages of differentiation (**Figure 1A, Materials and Methods**). We optimised the heat shock protocol to maximise the number of GSC-like cells entering differentiation, while minimising fly death due to heat stress.

Confocal microscopy was used to assign time points representing each stage from undifferentiated GSC to 16cc (terminal differentiation). We used the branching of the fusome (stained for alpha-spectrin)[49,50] to observe the progression of differentiation at each time point after heat shock (AHS) (**Figure 1B**). Based on this branching, we assigned each time point to an approximate stage of differentiation: 'no HS' (*bam* mutant), 5 hr (cystoblast, CB), 9 hr (2cc), 18 hr (4cc), 28 hr (8cc) and 38 hr (16cc) AHS (**Figure 1A**). This time course provides a framework for studying GSC differentiation, but it is important to note that we observed heterogeneity in cyst stages, which increased at later time points.

In *wild type* ovaries, Bam protein is not expressed in the GSC, but is upregulated during early differentiation[51]. To

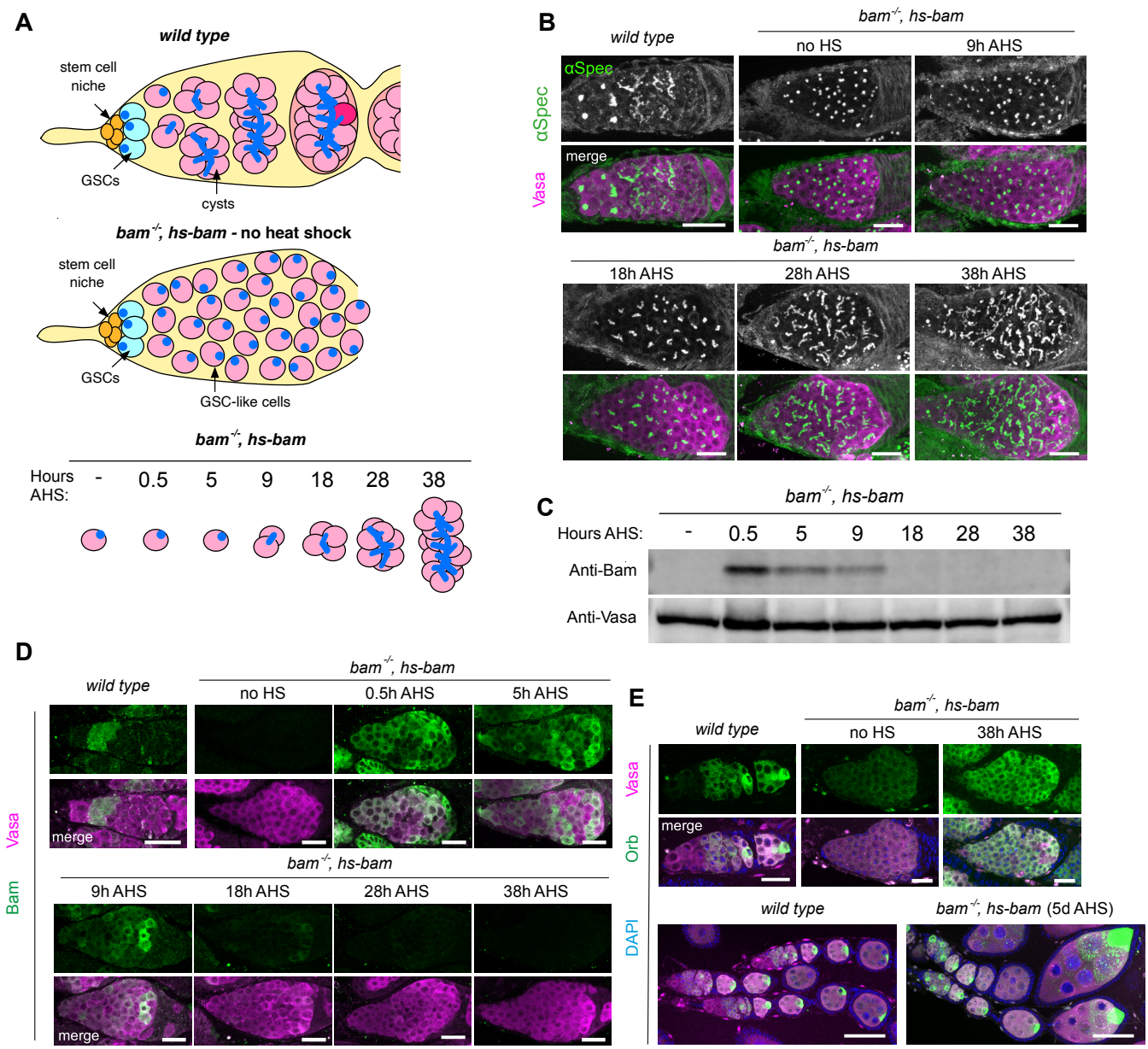

Figure 1 – Establishing a robust protocol to synchronise GSC differentiation *in vivo*

(A) Sketch illustrating *wild type* differentiation (top), and the accumulation of GSC-like cells in the *bam, hs-bam* ovaries used in the synchronisation experiment (middle). Heat shock induces Bam expression resulting in entry into differentiation, such that samples collected at the given times after heat shock (AHS) are enriched for particular stages of differentiation (bottom). **(B)** Example germaria from *wild type* or *bam, hs-bam* ovaries at the specified times AHS. Stained with immunofluorescence (IF) against α-spectrin (fusome, green and gray-scale) and Vasa (germline, magenta). **(C)** Western Blot using lysate from *bam, hs-bam* ovaries at specified times AHS. Probed for Bam (top) and Vasa (bottom). **(D)** IF against Bam (green) and Vasa (magenta) in germaria at given time points AHS. **(E)** IF against Orb (green) as a marker for terminal differentiation. DAPI (DNA, blue) and Vasa (magenta) are also stained. Scale bars in B, D and E (top) are 20 µm, in E (bottom) are 50 µm.

visualise the kinetics of Bam expression induced by our heat shock protocol, we performed Western Blot and immunofluorescence (IF) analyses across our time course. Performing Western Blots on whole ovaries revealed that Bam protein was strongly induced at 0.5 hr AHS and then declined to levels similar to those observed in the 'no HS' samples by 18 hr AHS (**Figure 1C**). To monitor the variation in Bam induction between cells that is not captured by Western blot analyses, we used IF, which revealed that the loss of Bam protein is variable at the cellular resolution: at 9 hr AHS, we observed a wider range of Bam intensity between differentiating cysts in comparison with 0.5 hr or 5 hr AHS (**Figure 1D**). While the basis of such variability has not been determined, it is possible that this explains the increasing heterogeneity of cyst development we observed by 38 hr AHS (**Figure 1B**).

To examine the progression of egg chamber development beyond terminal differentiation, we examined the expression of Orb, which is normally concentrated into the future oocyte during the 16 cell cyst stage[29]. IF revealed that Orb does not concentrate into a single cell of the 16cc by 38 hr AHS (**Figure 1E**), suggesting that this final time point captures the final stages of differentiation, prior to egg chamber formation. At 5 days AHS most egg chambers contain a single Orb positive cell and, as previously shown[43], females treated with our heat-shock protocol laid eggs that hatched and produced adult offspring. These findings confirm that normal germline development can be fully recapitulated in our synchronisation system.

Transcriptome measurements in synchronised differentiating GSCs reflect *wild type* differentiation

To examine mRNA expression during differentiation in synchronised GSCs, we performed RNA-seq on rRNA-depleted RNA extracted from *bam*$^{-/-}$*,hs-bam* ovaries collected at specified time points AHS (**Figure 1A**). We generated RNA-seq libraries from ovaries at 'no HS' (*bam* mutant) and 5 hr (CB), 9 hr (2cc), 18 hr (4cc), 28 hr (8cc) and 38 hr (16cc) AHS. Comparison between biological replicates showed that the data are highly reproducible (R^2>0.97).

To validate that the transcriptome measurements in the *bam*$^{-/-}$*,hs-bam* time course reflect mRNA accumulation during *wild type* differentiation, we used single molecule fluorescence *in situ* hybridisation (smFISH) to visualise mRNA transcripts in *wild type* germaria (**Figure 2A, S1A**). Marking the cell boundaries (phalloidin, F-actin) and the spectrosome and fusome (alpha-spectrin) enabled us to identify all the stages of differentiation in *wild type* ovaries. *vasa* mRNA is detected at ~ 200 FPKM throughout the RNA-seq time course, while *aubergine* (*aub*) mRNA is detected at a lower, but constant, level (~ 100 FPKM). Accordingly, using smFISH, we observed higher numbers of *vasa* mRNA transcripts in the cytoplasm of germ cells at all differentiation stages (**Figure 2Ai**), compared to *aub* mRNA (**Figure 2Aii**). *matrimony* (*mtrm*) mRNA presented levels below 10 FPKM until the 28 hr AHS time point, with a further increase at 38 hr AHS. This pattern of upregulation is also observed in *wild type* differentiation, with *mtrm* mRNA only observed in 8cc and 16cc (**Figure 2Aiii**). *bgcn* displays the opposite mRNA expression pattern, with declining mRNA levels in both the synchronised differentiating GSCs and *wild type* differentiation (**Figure 2Aiv**)[52]. Notably the synchronised differentiating GSC dataset recapitulates recently published mRNA expression patterns for *CG32814,* which is reported to be downregulated after the GSC[41], and *blanks*, which is downregulated at the 8cc stage[36] (**Figure S1A**). Collectively, validations by smFISH indicate that the RNA-seq data in synchronised differentiating GSCs mirrors what is observed in *wild type* ovaries both in terms of mRNA levels and changes during differentiation. The smFISH experiments suggest that an expression level in the RNA-seq below 10 FPKM corresponds to a very small number of mRNA transcripts that is only sporadically detected in cells, so we set this as the threshold for further analysis. In our RNA-seq data, 6532 genes were expressed at > 10 FPKM in at least one time point.

With the advent of single cell sequencing technologies, others have recently used single cell (sc)RNA-seq analysis to characterise different cell types in adult *Drosophila* ovaries[38–40]. For instance, Rust et al. used pseudotime analysis to identify transcriptional signatures, with 12 'marker genes' representing different stages of germline development. As additional validation of our dataset, we compared these data to our bulk RNA-seq from the synchronised GSCs and found that our dataset is consistent with the pseudotime analysis inferred from scRNA-seq (**Figure S1B**), but with increased sequencing depth.

An important caveat is that the protocol used to drive Bam expression is also expected to induce acute changes in the expression of the heat shock responsive genes[53]. Transcript level changes of the heat shock responsive genes are characterised by their transient nature, quickly dampening over short periods after the stimulus is removed. To identify genes with acute changes in mRNA level upon heat shock treatment, we generated RNA-seq libraries from ovaries at 0.5 hr AHS. 68 genes underwent a significant > 3-fold change in transcript level in the 0.5 hr AHS time point compared to 'no HS' (with > 10 FPKM expression in at least one of these time points). Most of these genes recovered towards the 'no HS' level during the time course, but at differing rates (**Figure S1C**). Gene ontology analysis showed that this cohort of genes were highly enriched for heat response and protein folding terms (**Figure S1D**). Therefore, this small subset of genes, along with an additional 20 contaminant genes (encoding proteins of the chorion and vitelline membrane, which are produced by somatic cells), were excluded from downstream analysis (**Table 1**). This filtering resulted in a dataset of 6444 genes expressed during the time course (**Figure 2B, Table 2**).

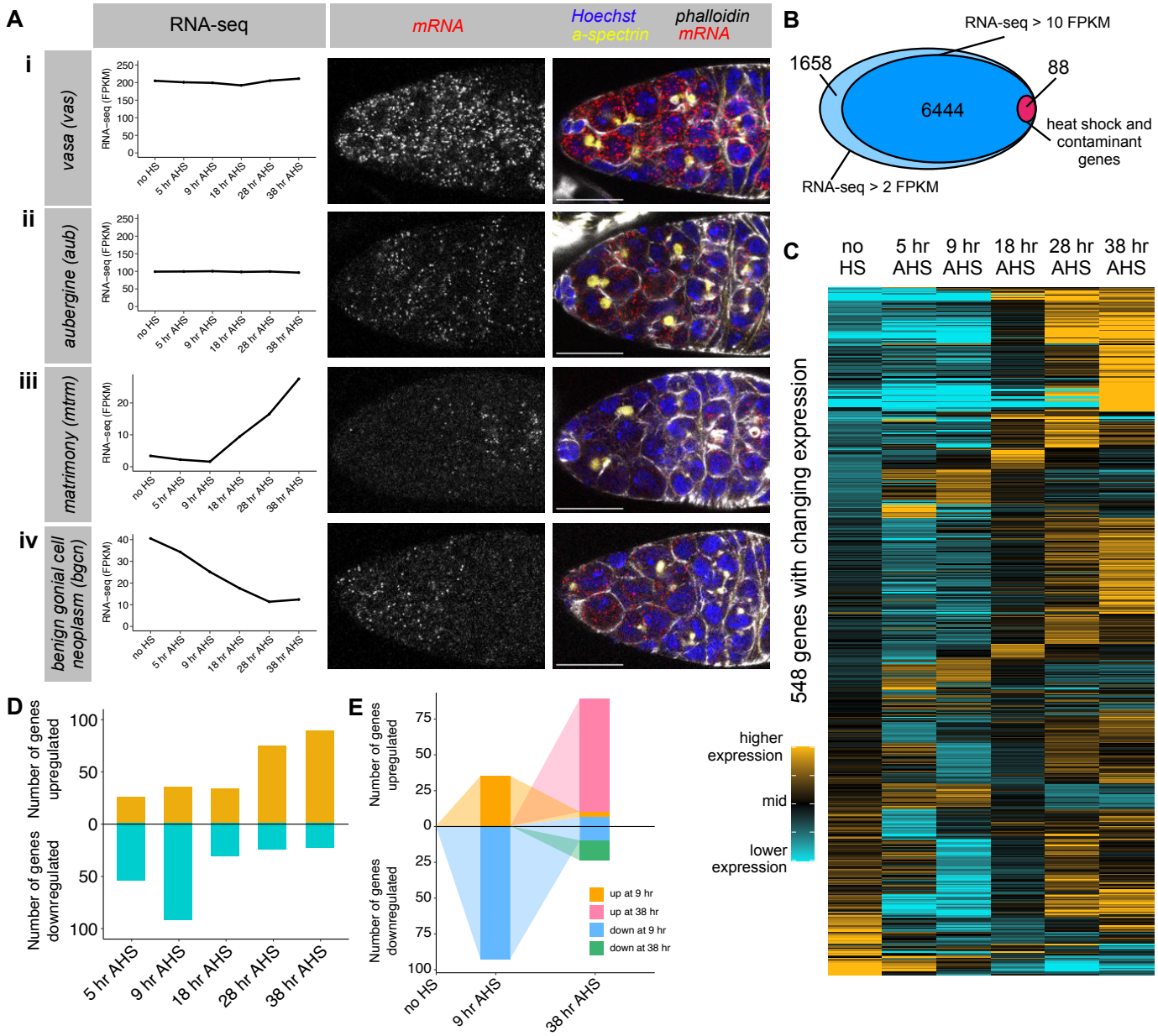

Figure 2 – RNA-seq in synchronised differentiating GSCs reveals dynamic changes in the transcriptome
(A) single molecule fluorescent *in situ* hybridisation (smFISH) was used in *wild type* germaria (right) to validate the RNA expression measurements in the synchronised differentiating GSC RNA-seq dataset (left). *Wild type* germaria are stained for DNA (Hoechst, blue), actin (phalloidin, gray), fusome (α-spectrin, yellow), and mRNA transcript of interest (smFISH, red and grayscale): **(i)** *vas*, **(ii)** *aub,* **(iii)** *mtrm* and **(iv)** *bgcn*. Scale bars are 15 µm. **(B)** RNA-seq in the differentiating GSCs detected 8177 genes expressed at least 2 FPKM at one time point (excluding the 0.5 hr heat shock sample), and 6535 of these were expressed to at least 10 FPKM. 90 genes were excluded due to a strong heat shock effect or chorion contamination. **(C)** Heatmaps illustrating RNA-seq expression level across the time course. Each row represents one gene of the 548 genes that exhibit a significant 1.6-fold change in expression between two time points. Expression level is scaled per gene such that black represents the mean expression across the time course, gold represents a 25% higher expression than the mean, and cyan represents a 25% lower expression than the mean. Genes were grouped by fold change in mRNA expression, starting with the final time point. **(D)** Number of genes with a significant 1.6-fold change at each time point compared to 'no HS'. Gold = upregulation, cyan = downregulation. **(E)** Illustrating the overlap between genes with significant up or down regulation at 9 hr AHS and 38 hr AHS. Orange and blue represent genes with changing expression at 9 hr AHS, and these are followed to 38 hr AHS. Additional genes with changing expression at 38 hr AHS are coloured pink and green.

GSC differentiation involves dynamic changes in the transcriptome

Having established that the synchronised GSC RNA-seq dataset parallels what is observed during *wild type* differentiation, we aimed to identify the set of genes for which mRNA levels change during GSC differentiation. To do so, we performed differential expression analysis and found 548 genes (~ 8.5% of expressed genes) with a significant ($p < 0.05$) and greater than 1.6-fold difference in mRNA level between any two time points (in which the expression was > 10 FPKM in one of the compared time points, and excluding the 0.5 hr AHS sample) (**Figure 2C**). Comparing to 'no HS', we found that most mRNA downregulation (65%) is observed at the 5 hr and 9 hr AHS time points (CB and 2cc), while most upregulation (64%) is observed at the 28 hr and 38 hr AHS time points (8cc and 16cc) (**Figure 2D**). Strikingly, we found that most genes (84%) that are up or downregulated at 9 hr AHS (2cc) returned to 'no HS' levels by 38 hr AHS (16cc) (**Figure 2E**), which is inconsistent with a model of gradual accumulating changes from GSC to 16cc. In contrast, the majority (82%) of mRNA expression changes at 38 hr AHS are contributed by genes which exhibited no significant (>1.6-fold) change at 9 hr AHS. These data reveal two waves of dynamic changes in the transcriptome throughout differentiation, potentially underlying the different cellular changes occurring at different stages of differentiation.

To characterise the observed changes further, we asked which genes contribute to each wave of mRNA expression change, and performed gene ontology analysis. We considered genes with mRNA level changes at 9 hr AHS (2cc) and at 38 hr AHS (16cc) in comparison to 'no HS' (**Figure S2A**). We found that the group of genes upregulated at 9 hr AHS was enriched for genes involved in DNA replication and the cell cycle (**Figure S2Bi**), while downregulated genes were enriched for genes involved in regulation of lipid storage. At 38 hr AHS the upregulated genes were enriched for annotations of the polar granule (GOterm: P granule) (**Figure S2Bii**), which are assembled during oogenesis[54], with no significant enrichment for downregulated genes. At 38 hr AHS, the upregulated group includes genes known to play a role in meiosis (*mtrm, c(3)g, orb, corolla*) and oocyte development or early embryogenesis (*osk, bru1, dhd, png, alphaTub67C*), while the downregulated group of genes includes *bgcn, blanks, RpL22-like* and *eIF4E3*.

Splicing analysis reveals changes in exon inclusion and promoter usage during differentiation

Differential expression analysis at the gene annotation level obscures changes in mRNA splicing, which can alter the encoded protein isoform. Therefore, we quantitated changes in splicing independently of changes in mRNA expression level by pair-wise analysis of our RNA-seq datasets using JUM[55]. The resulting measurement of deltaPSI (percent spliced in) describes the change in the usage of each splicing event between two conditions. Overall, we observed a large number of splicing changes, with different genes changing in splicing in the early wave (9 hr AHS) compared to the late wave (38 hr AHS) (**Figure 3A**).

Our analysis identified both known and novel examples of splice isoform changes that modify the encoded proteins during differentiation. Over-expression of isoform-specific cDNA constructs has been used previously to infer that a burst of cytoplasmic Rbfox1 during late GSC differentiation is caused by a change in splice isoform to exclude the nuclear localisation signal (*Rbfox1-RN/F* isoform annotated by FlyBase)[17]. In our GSC differentiation time course, this alternative splicing event is captured and is most pronounced at 28 hr AHS (**Figure 3B**). Hu li tai shao (Hts) is a key component of the fusome, and is required for coordinating cyst division and oocyte specification[56]. *hts* does not show a significant change in mRNA expression level during our GSC differentiation time course, but alternative splicing analysis shows a change in splicing at the 3' end of the transcript, producing alternative protein isoforms. During differentiation, the ratio of 3' end usage shifts such that *hts-RO/R/S/Q/L/M* (*adducin,* encoding a conserved F-actin and Spectrin-binding protein) and *hts-RA/K/N* (*ovhts*) are increased at 38 hr AHS compared to 'no HS' (**Figure 3C**)[57,58]. The encoded Ovhts polyprotein is cleaved to release HtsRC, which specifically localises to the ring canals during cyst development, therefore our data shows that HtsRC production is upregulated at the level of alternative splicing. The mRNA isoform *hts-RP* was thought to be testis-specific[58] but is quite highly expressed in the 'no HS' sample and is downregulated during our time course. Hence, developmentally regulated alternative splicing can lead to functional changes to the protein isoforms expressed in the cell without a change in overall gene expression level, revealing a layer of regulation during GSC differentiation that has not yet been systematically explored.

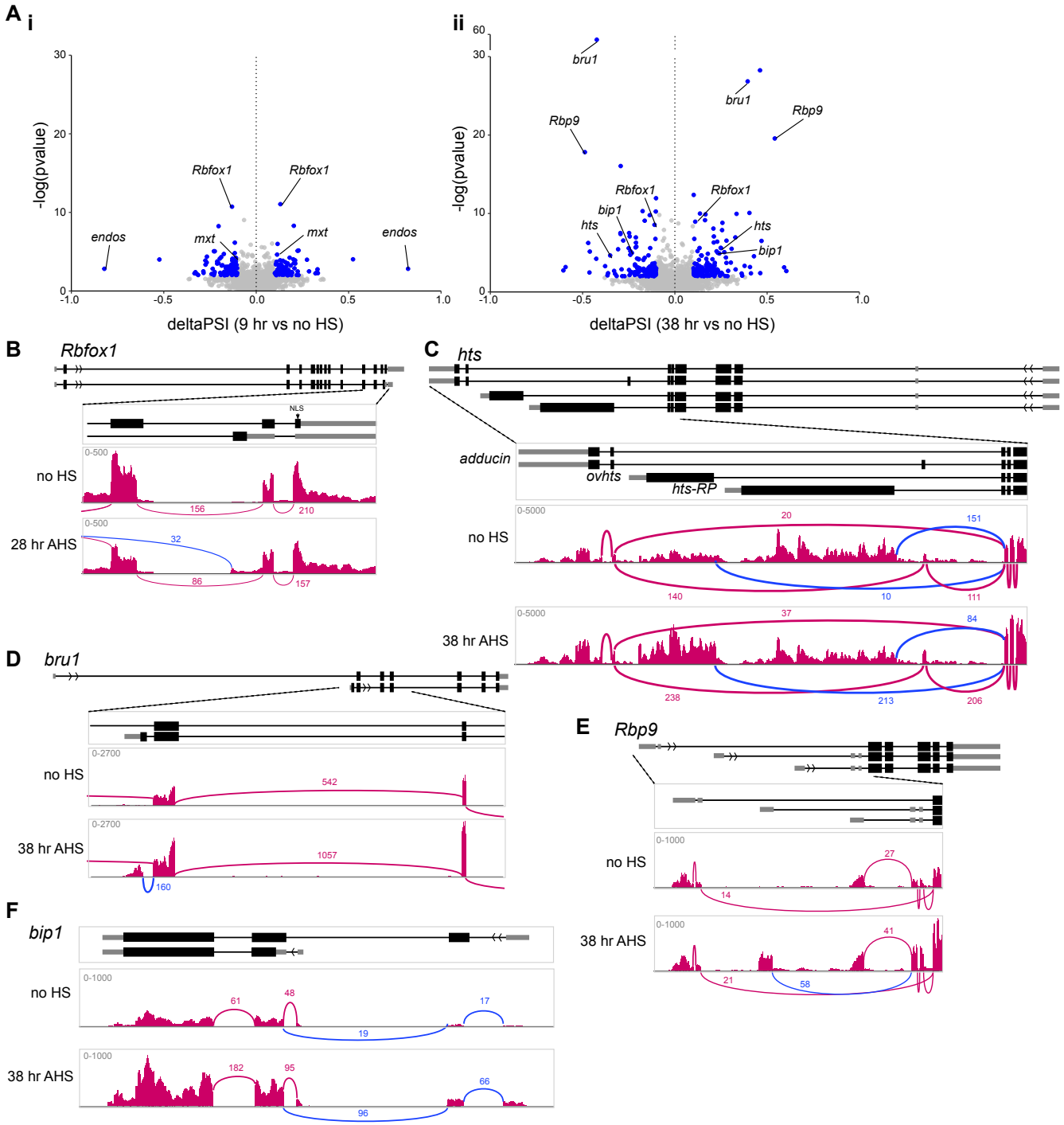

Figure 3 – Changes in splicing during differentiation can alter regulation or protein isoform
(A) Splice site usage at 9 hr AHS **(i)** or 38 hr AHS **(ii)** compared to 'no HS', plotted as deltaPSI (percent spliced in). Blue points meet the thresholds of >0.1 or <-0.1 deltaPSI and $p < 0.01$. **(B-F)** Example changes in splicing of *Rbfox1* **(B)** and *hts* **(C)**, as well as transcription start site usage of *bru1* **(D)**, *Rbp9* **(E)** and *bip1* **(F)**. Simplified gene structure is shown above, and RNA-seq read tracks from IGV are shown with Sashimi plots to visualise splice junctions. Changing splicing of interest is highlighted in blue.

Unexpectedly, splicing analysis also provided insight into the mechanism of regulation of genes that exhibit changing expression level during differentiation. We found that *bruno* (*bru1*), encoding an RBP that functions to inhibit the expression of the mitotic cyclins after meiotic entry[59], is expressed in the GSC and upregulated during differentiation, but that this regulation occurs through the activation of an additional downstream transcription start site (TSS) (**Figure 3D**). In the 'no HS' sample, the majority of transcription initiates at the most 5' start site (producing the *bru1-RK* transcript), while at 38 hr AHS, a downstream TSS is also active, producing the *bru1-RA/E* transcripts, which likely underlies the upregulation of Bru1 protein observed during

differentiation. Similarly, *Rbp9,* encoding another RBP required for proper cyst differentiation and oocyte determination[60], is also upregulated during differentiation. Splicing analysis uncovered the activation of an additional TSS to express the *Rbp9-RB/E/G/J* transcripts at 38 hr AHS (**Figure 3E**). In the examples of *bru1* and *Rbp9*, changes in TSS usage lead to the use of different 5' untranslated sequences (5' UTR) without a change in coding sequence. Lesser-studied genes include *bip1,* which is also upregulated during GSC differentiation and shows specific increased transcription from an upstream TSS at 38 hr AHS to produce *bip1-RA* (**Figure 3F**). In this case, differential TSS usage is expected to lead to the expression of different protein isoforms. Altogether, these examples illustrate how activation of an alternative TSS is a mechanism to upregulate gene expression.

Ribo-seq captures translation dynamics during GSC differentiation

RNA-seq measures gene expression changes at the mRNA level, which are often thought of as a proxy for consequential changes at the protein and cell fate level. Indeed, scRNA-seq has been broadly used as a readout for fate changes[61–64]. This premise assumes no change in the translation efficiency of the transcripts, but mounting evidence indicates that transcripts for different genes are not equally translated[65]. Translation regulation plays a significant role during GSC differentiation - indeed the master differentiation factor Bam is itself a regulator of translation[12,15]. Despite this, the dynamics of translation changes during stem cell differentiation are unknown, largely due to the large amount of material required to analyse translation genome-wide. To circumvent these difficulties, we applied the *bam*$^{-/-}$*,hs-bam* system to obtain enough starting material to perform Ribo-seq at the same time intervals as the RNA-seq dataset. Even using the synchronisation approach, the amount of tissue was limited compared to previous Ribo-seq experiments in *Drosophila* S2 cells[66,67], embryos[68], oocytes[69] or ovaries[70], so we first performed quality control analysis on the Ribo-seq libraries (**Figure S3**). Comparisons between biological replicates revealed that the data is highly reproducible (R^2>0.97). As expected from high quality Ribo-seq data, we observed that the majority of the reads (58-70%) showed the expected ribosome footprint (28-32nt long), overwhelmingly mapped to the sense direction of the CDS (>90%) or 5' UTR (~8.9%) and showed a strong 3-nucleotide P-site periodicity. This benchmarking confirms that our Ribo-seq is of high quality despite the limitations in input material.

We assessed the translation of the 6444 genes that we had determined to be expressed by RNA-seq (**Figure 4A, Table 3**). Of these, 43 further genes showed heat shock effects in the Ribo-seq (> 3-fold change in the 0.5 hr AHS sample compared to 'no HS'). Using a threshold of 10 FPKM in the Ribo-seq, we found that 5922 of the expressed genes were translated at some point during our time course, while 479 genes were not translated at any time point (< 10 FPKM).

Just as we validated the RNA-seq datasets against *wild type* differentiation using smFISH, we aimed to validate the Ribo-seq through independent approaches. We first compared the Ribo-seq reads for *bam* to the results we obtained by Western Blot (**Figure 1C**). From the Ribo-seq, we found that *bam* translation peaks at 0.5 hr AHS, but declines gradually (**Figure 4B**), which matches the Western Blot. We then focused on hallmark genes that have been previously characterised as being translationally regulated during GSC differentiation. For instance, *osk* mRNA, which is crucial for assembly of the germplasm at the posterior pole of oocytes, is not transcribed until the late stages of GSC differentiation, but remains translationally repressed in differentiated cells until much later in oogenesis[28,71,72]. In agreement, the RNA-seq data revealed a progressive increase in the level of *osk* mRNA from 18-38 hr AHS (4cc to 16cc), while the Ribo-seq showed that *osk* mRNA was not engaged with ribosomes throughout the time course (**Figure 4Ci**). On the other hand, transcriptional reporters suggested that the *nos* gene is transcribed throughout GSC differentiation, while the protein level decreases during the CB to 4cc stage[15]. The Ribo-seq data revealed a sharp decrease in *nos* translation at the 5 hr and 9 hr AHS time points (CB to 2cc), but surprisingly, the mRNA level mirrored this change, which together with constant transcription implies decreased mRNA stability (**Figure 4Cii**). Both the RNA-seq and Ribo-seq showed full recovery of *nos* by 28 hr AHS (8cc).

While our datasets recapitulate examples of translation regulation already shown in the literature, we wanted to validate the Ribo-seq in an unbiased manner. To do so, we selected genes with similar RNA expression levels but different Ribo-seq read levels and procured FlyFOS GFP-tagged transgenic lines. The FlyFOS transgenes are expected to recapitulate the expression of the endogenous gene, as they were designed with the goal to include all regulatory sequences existing on endogenous genomic loci[73]. We stained germaria with *gfp* smFISH to measure RNA level, and GFP protein to measure the

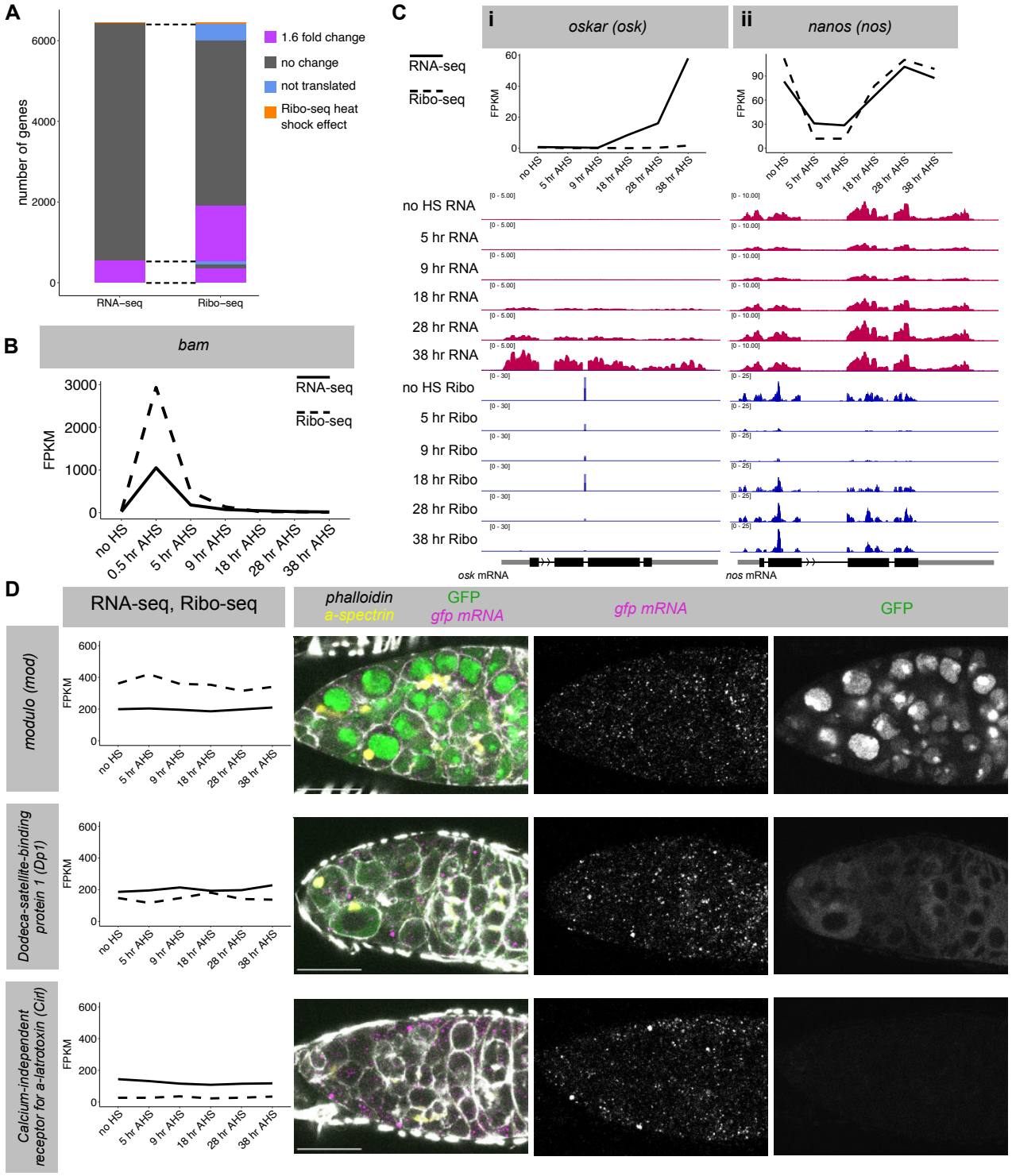

Figure 4 – Ribo-seq in synchronised differentiating GSCs recapitulates changes in translation during normal differentiation

(A) After filtering, 6444 genes are expressed at >10 FPKM in at least one time point by RNA-seq. 548 of these genes show a >1.6-fold change between any two samples. Of these 548 genes, 353 also show a 1.6 fold change in Ribo-seq reads between two samples. 1360 genes show a >1.6-fold change in the Ribo-seq with no significant change in the RNA-seq. **(B)** *bam* transcript level and translation during the time course from RNA-seq and Ribo-seq data (FPKM). **(C)** RNA-seq and Ribo-seq in the synchronised GSC system recapitulates previously characterised regulation of *osk* **(i)** and *nanos* **(ii)**. IGV tracks for each time point for RNA-seq (red) and Ribo-seq (blue). **(D)** GFP-tagged FlyFOS constructs (*modulo, dodeca satellite-binding protein 1, calcium-independent receptor for a-latrotoxin)* stained for *gfp* smFISH (magenta and individual grey scale) and GFP protein (green, and individual grey scale), f-actin (phalloidin, grey scale) and fusome (α-spectrin, yellow). Scale bars are 15 µm. graphs: solid line = RNA-seq, dashed line = Ribo-seq

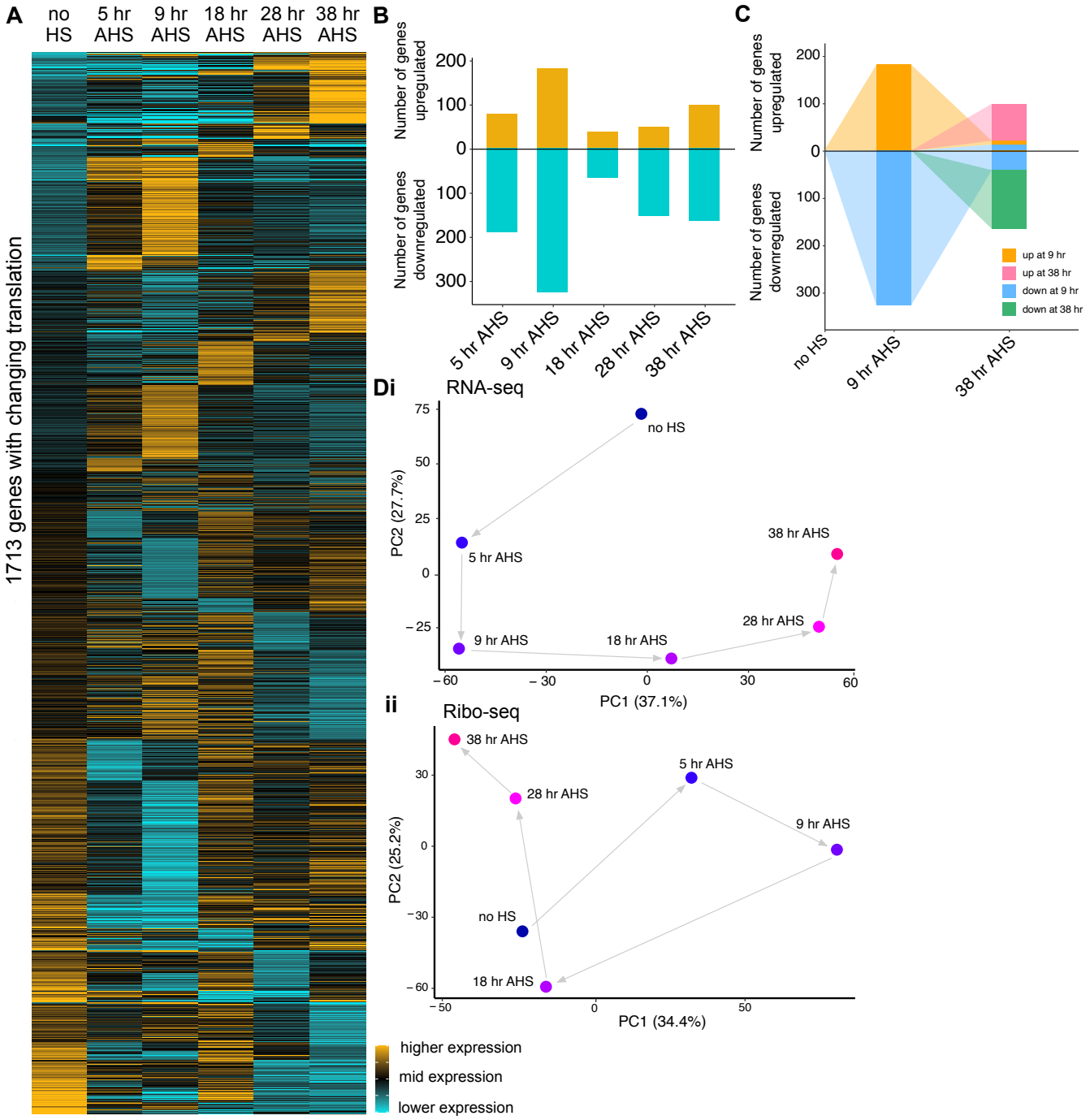

Figure 5 – Ribo-seq in synchronised differentiating GSCs uncovers changes in translation during differentiation

(A) Heatmap illustrating translation level across the time course. Each row represents one gene of the 1713 genes that exhibit a significant 1.6-fold change in translation between any two time points. Expression level is scaled per gene such that black represents the mean translation (Ribo-seq FPKM) across the time course, gold represents a 25% higher translation than the mean, and cyan represents a 25% lower translation than the mean. Genes were grouped by fold change in Ribo-seq, starting with the final time point. **(B)** Number of >1.6-fold changes in Ribo-seq at each time point compared to 'no HS'. Gold = upregulation, Cyan = downregulation. **(C)** Illustrating the overlap between genes with significant up or down regulation in the Ribo-seq at 9 hr AHS and 38 hr AHS. Orange and blue represent genes with changing expression at 9 hr AHS, and these are followed to 38 hr AHS. Additional genes with changing expression at 38 hr AHS are coloured pink and green. **(D)** PCA of the RNA-seq **(i)** and Ribo-seq **(ii)** in the differentiating GSC time course.

level of each fusion protein (**Figure 4D**). Using the same *gfp* smFISH probes and anti-GFP antibody minimises confounding detection effects. In agreement with the RNA-seq data, the smFISH showed similar numbers of mRNA transcripts for each gene. Moreover, mirroring the results from the Ribo-seq analysis, the GFP protein

levels were very different for each gene (highest = *mod*, medium = *Dp1*, lowest = *Cirl*). Therefore, we conclude that the Ribo-seq in synchronised differentiating GSCs reflects changes in translation during *wild type* differentiation. Ribo-seq data reports the rate of protein production during differentiation, providing more direct insight into the changes in protein complement during differentiation compared with RNA-seq.

Ribo-seq identifies global remodelling of translation during GSC differentiation

We asked if changes in mRNA expression corresponded to changes in the Ribo-seq. 548 genes showed a >1.6-fold change in RNA level between any two time points, and 353 of these (64%) also showed a significant 1.6-fold change between two samples in the Ribo-seq dataset (**Figure 4A**). However, an additional 1360 genes showed a change in the Ribo-seq but not the RNA-seq data, revealing that these genes are regulated primarily at the level of translation. In total, 8.5% of transcribed genes show a >1.6-fold change in RNA expression at some point over the time course, while 29% of translated genes show a >1.6-fold change in the Ribo-seq experiment. This result illustrates that a more extensive remodelling of the translatome than the transcriptome is at play during GSC differentiation.

In total, 1713 genes showed a >1.6-fold difference in translation level between any two time points (excluding the 0.5 hr AHS sample) (**Figure 5A**). Comparing the 38 hr AHS time point to 'no HS', 99 genes were upregulated, including *orb, grk, moon, png, c(2)M, bru1, alphaTub67C* and *Rbp9,* while 165 were downregulated at the level of translation, including *bgcn, stau* and *Pxt.* There were roughly twice as many downregulated genes as upregulated genes at each time point, with two waves of changes around an inflection point at 18 hr AHS (**Figure 5B**). Similarly to the RNA-seq analysis, we found that the majority (88%) of genes that increase or decrease in translation in the early wave (9 hr AHS, 2cc), returned to 'no HS' levels by 38 hr AHS (16cc) (**Figure 5C**). The majority (77%) of translation changes in the late wave are contributed by genes that exhibited no change in the early wave.

We performed gene ontology analysis and found that, as in the RNA-seq, the first wave of upregulation was enriched for genes involved in cell cycle and DNA replication, as well as cytoskeleton organisation (**Figure S4A, S4B**). The early wave of downregulation in the Ribo-seq was enriched for genes involved in translation, primarily the ribosomal proteins, suggesting that the previously observed downregulation of ribosome biogenesis during GSC differentiation[24,25] is itself regulated at the level of translation. There was no significant enrichment in the second wave at the level of translation. Indeed, many of the upregulated transcripts that are enriched in the polar granules are translationally repressed at this stage, as for *osk*.

To get a global perspective of the changes occuring at the transcriptome and translatome level, we used Principal Component Analysis (PCA) to examine the variance in the RNA-seq and Ribo-seq samples throughout our time course (**Figure 5D**). In the RNA-seq, PC1 explains ~37% of the variance, in which the 9 hr AHS and 38 hr AHS samples are the most separated. Illustrating an inflection point around 18 hr AHS, this sample was the most similar to the 'no HS' sample. PC2 explains ~28% of the variance and groups the mid samples (9 hr AHS, 18 hr AHS and 28 hr AHS) closer together. In the Ribo-seq samples, PC1 explains ~34% of variance and again shows the biggest difference between 9 hr AHS and 38 hr AHS, with 'no HS' and 18 hr AHS positioned close to each other. Thus, globally, our data reveal that both the transcriptome and translatome undergo two waves of remodelling during differentiation.

Transcripts that are translationally repressed during differentiation are often translated later during oocyte or embryo development

A cohort of genes are expressed but translationally repressed throughout our time course, so we asked whether they are translated later in development rather than reflecting spurious transcription. To explore this hypothesis, we examined the expression and translation of these genes in previously published RNA-seq and Ribo-seq experiments using the whole ovary as input[74] (NCBI BioProject PRJNA466150). Whole ovary datasets primarily represent expression and translation in maturing egg chambers, which make up the bulk of the tissue. We focussed on two groups of untranslated genes from our time course (<10 FPKM in the Ribo-seq throughout the time course): firstly the 'upregulated' group (>1.6-fold increase in RNA level from 'no HS' to 38 hr AHS, 30 genes, **Figure 6A** blue points), and secondly the 'constitutive' group (>15 FPKM at every time point of the RNA-seq, 129 genes, **Figure 6A** purple points).

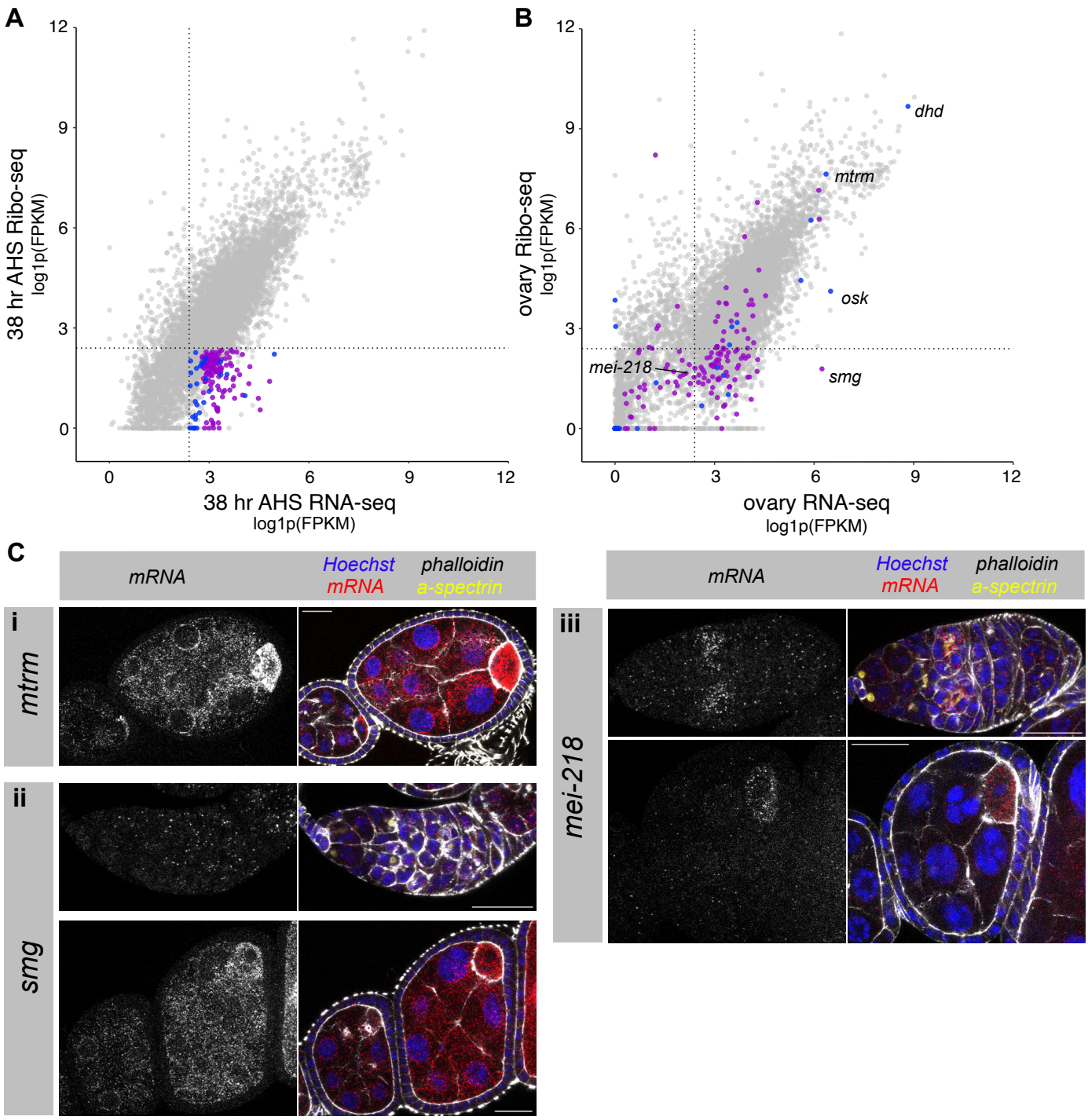

Figure 6 – Translationally repressed genes during differentiation are often translated later in egg chamber or embryo development

(A) FPKMs for each gene in the RNA-seq and Ribo-seq datasets at 38 hr AHS, plotted as log1p(FPKM). Highlighted genes are untranslated (<10 FPKM throughout the time course). Blue represents upregulated genes (>1.6 fold increase in RNA level from 'no HS' to 38 hr AHS), purple represents constitutive genes (>15 FPKM in the RNA-seq at every point of the time course). Dotted lines represent 10 FPKM. **(B)** Plotting log1p(FPKM) in whole ovary RNA-seq and Ribo-seq (Greenblatt & Spradling, 2017). Genes coloured as in A. Dotted lines represent 10 FPKM. **(C)** smFISH in *wild type* ovaries for **(i)** *mtrm*, **(ii)** *smg* and **(iii)** *mei-218. wild type* ovarioles are stained for DNA (Hoechst, blue), actin (phalloidin, gray), fusome (α-spectrin, yellow), and mRNA transcript of interest (smFISH, red and grayscale). Scale bars are 20 µm.

Analysis of the mRNA expression and translation of the 'upregulated' group (30 genes) revealed that 12 of these genes were expressed to >10 FPKM in the whole ovary RNA-seq, and of those, 8 were translated to >10 FPKM in the whole ovary Ribo-seq (**Figure 6B**, blue points). This group includes *osk*, which has been shown to be loaded into the developing oocyte and translated at the posterior pole[28,71,72], as well as meiosis genes (including

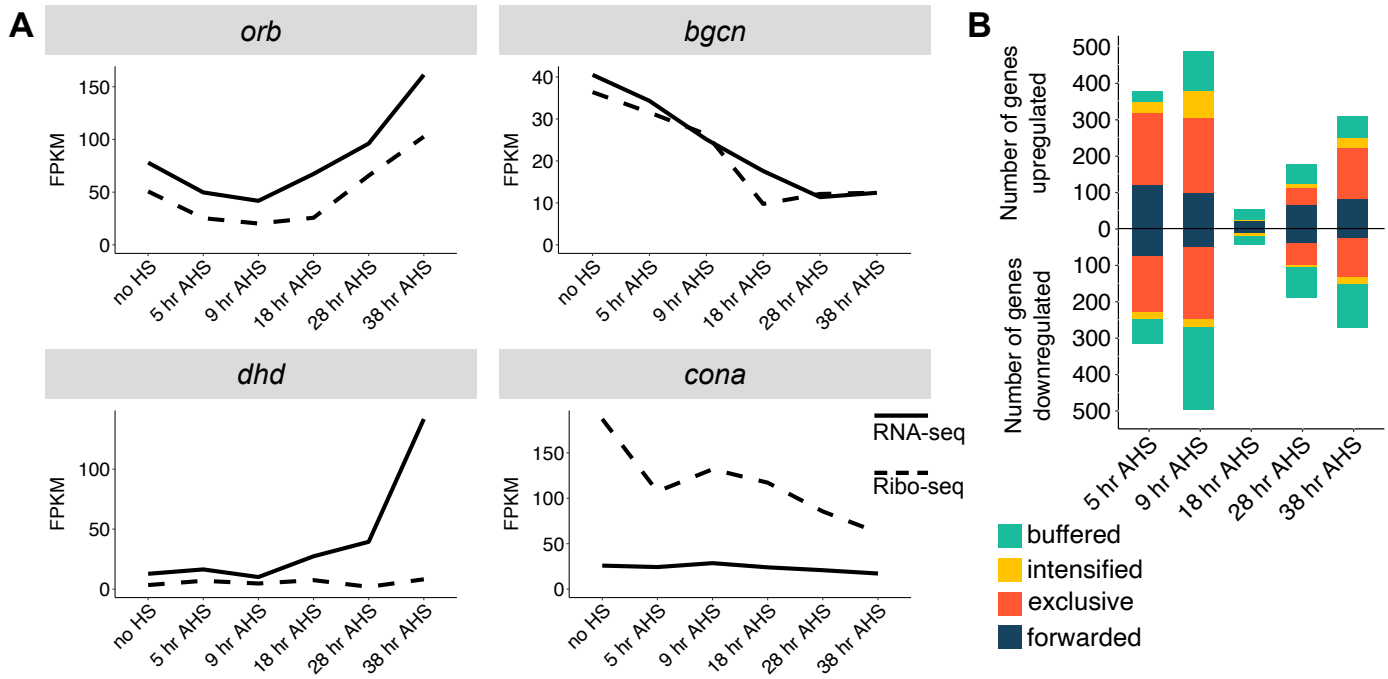

Figure 7 – Transcript level changes can be intensified or buffered at the level of translation through regulation of translation efficiency

(A) Changing expression of different genes in the RNA-seq (solid line) or Ribo-seq (dashed line). Ribo-seq in *orb* and *bgcn* reflects the RNA-seq, but for *dhd* and *cona* there is additional regulation at the level of translational efficiency. **(B)** Number of genes classified into each of four regulatory groups (forwarded, exclusive, intensified or buffered) at each time point compared to 'no HS'. Up or downregulation is classified by the direction of change in Ribo-seq.

dhd, mtrm (**Figure 6Ci**) and *wisp*), and *yolkless* (*yl*), which is involved in vitellogenesis of the egg[75].

Of the 'constitutive' group of genes, 90 were expressed to >10 FPKM in the whole ovary RNA-seq (**Figure 6B**, purple points). 30 of these were also translated to >10 FPKM in the whole ovary Ribo-seq, including *giant nuclei* (*gnu*), which regulates the PNG kinase complex driving the early embryonic nuclear divisions[76]. The remaining 60 genes remain translationally repressed, including the RBP-encoding gene *smaug* (*smg*), which is known to be loaded as mRNA into the oocyte and is translationally repressed until egg activation, downstream of the PNG kinase[77]. Our data shows that *smg* mRNA is expressed throughout early GSC differentiation (**Figure 6Cii**), and so the translation repression mechanism must be active throughout differentiation and oogenesis. In this case, a robust translational repression mechanism may make any additional transcriptional regulation obsolete.

We hypothesised that some genes that are translationally repressed during GSC differentiation but not expressed in the whole ovary RNA-seq, might be translated at a specific stage of egg chamber development but fall beneath the detection threshold in the whole ovary datasets. Indeed several genes expressed only during the first stages of differentiation in our dataset (e.g. *blanks, bgcn*), are not detected >10 FPKM in the whole ovary RNA-seq. For example, *mei-218,* which encodes a protein involved in meiotic recombination[78], is not translated in our GSC differentiation time course, and does not meet the detection threshold in the whole ovary RNA-seq. We performed smFISH and showed that *mei-218* mRNA is expressed throughout the germarium and upregulated at the 16cc stage (**Figure 6Ciii**). *mei-218* mRNA is then downregulated but continues to be lowly expressed in developing egg chambers with enrichment in the oocyte. This is consistent with published *in situ* and antibody stainings showing that Mei-218 protein is upregulated in the 16cc during meiotic prophase[78]. These examples illustrate that translational repression is implemented widely during GSC differentiation to prepare the pool of transcripts in advance of a change of fate during development.

Transcript level changes can be intensified or buffered at the level of translation through regulation of translation efficiency

Accumulating evidence indicates that changes in the translatome are a composite of differences in mRNA level and differences in translation efficiency (TE) of

each gene. TE is a measure that is proportional to ribosomes per transcript, and can be calculated for each gene as Ribo-seq reads divided by RNA-seq reads. When considering individual examples in our dataset, we find cases in which the changes in translation reflect similar changes in mRNA level, e.g. *orb* and *bgcn*, but for others the Ribo-seq is not paralleled by the RNA-seq (e.g. *osk* and *dhd*), implying that the latter group is regulated at the level of TE (**Figure 4C, 7A**). In the case of *corona* (*cona*), a gene encoding a component of the synaptonemal complex required for chromosome pairing, both transcription and translation decrease during differentiation, but the effect is much greater at the level of translation. To systematically and quantitatively determine the changes in TE for each gene, we applied deltaTE[79] on RNA-seq and Ribo-seq data throughout our time course compared to 'no HS'. With a threshold of >1.6 fold change in TE (with p value <0.05 and FPKM of at least 10 in one of the compared RNA-seq samples), we identified 874 genes with changing TE during the time course (**Figure S5**).

To understand the different types of gene regulation in more detail, we grouped genes into four classes[79]: regulation only at the mRNA level (forwarded), only at the level of translation efficiency (exclusive), or by mRNA and translation efficiency changing in the same direction (intensified) or opposite directions (buffered). We classified gene regulation into these four categories at each time point relative to the 'no HS' sample. Overall, we found that translation regulation contributed to the regulation of more genes than mRNA level, with the exception of the 18 hr AHS time point where 96% of regulatory events involved changing mRNA level (**Figure 7B**). Although 'intensified' represents the most effective way to change protein expression, at each time point, only 4-10% of regulatory events are classified as such. Perhaps this finding reflects the complexity of establishing mechanisms for both transcriptional and translational regulation on any given gene. On the other hand, the 'buffered' category - in which translation control neutralises the changes in mRNA levels - was much larger, at each time point making up 14-56% of regulatory events. In these cases, changing TE maintains the status quo at the level of translation, while the transcriptome is remodelled, perhaps in preparation for the coming stages of differentiation. These results emphasise that changes in mRNA level are a less consequential output than measurements obtained by Ribo-seq, and that translation efficiency is a major lever to regulate protein expression during germline stem cell fate transitions.

Discussion

During differentiation, stem cell progeny undergo a fate change that can transform cellular morphology, metabolism and function. The reproducibility of development and homeostasis in general, and of germline stem cell differentiation in our particular case, suggests that the orchestration gene expression during fate changes is tightly regulated. Many key regulators have been identified driving GSC differentiation, but an understanding of downstream changes in gene expression has been hindered due to technical limitations of studying a small number of cells at specific stages of differentiation in a complete adult tissue. We have developed a protocol to synchronise GSC differentiation *in vivo*, allowing us to collect tissue samples representing the progression through differentiation. This method generates sufficient material to perform RNA-seq and Ribo-seq at high resolution throughout GSC differentiation, providing a rich insight into the remodelling of the transcriptome and translatome during this cell fate change.

We performed benchmarking analysis to confirm the quality and reproducibility of our sequencing datasets, and thoroughly validated them against normal *wild type* differentiation in comparison to the published literature and using orthogonal imaging-based methods. The RNA-seq data of synchronised differentiating GSCs reproduces the gene expression patterns identified through scRNA-seq[38–41], and the increased depth of the data provided by RNA-seq allowed us to identify more differentially expressed genes in our dataset. Importantly, we found that the translatome undergoes 3-fold more changes than the transcriptome during GSC differentiation, which could explain why it has been difficult to specifically distinguish signatures for each stage of differentiation from scRNA-seq data. While the role for translation control is not surprising, given that translation regulators have been shown to be drivers of GSC differentiation[15,17,80], the magnitude of the effect was not anticipated. Importantly, we found that changes in mRNA level were not predictive of changes in translation: just a third of the observed changes in the RNA-seq also show a concomitant change in the Ribo-seq. This finding is in line with previous reports that transcript level (as measured by RNA-seq) is not a good proxy for protein level[65]. RNA-seq enables insight into the regulatory processes upstream of protein production, but on its own provides limited explanation of the cell biological changes happening during cell fate transitions.

While we found hundreds of changes in gene expression at the level of the transcriptome and translatome, gene ontology enrichment analysis uncovered fewer enriched terms than we expected. This may be because the activity of any particular pathway can be regulated by the level of one limiting component. Early in differentiation there was an upregulation of genes involved in the cell cycle and DNA replication, which may drive the four mitotic divisions that occur during differentiation. Later in differentiation, this group of genes are no longer upregulated. It has been previously proposed that when the RNA-binding protein Bruno (Bru1) is expressed late in differentiation, it translationally represses mitotic factors leading to exit from the cell cycle[59,81,82]. In contrast, our findings suggest that many cell cycle factors are regulated primarily at the mRNA level, not at the translation level. During early differentiation, the downregulated genes in the Ribo-seq were enriched for terms involving the ribosome, regulated by decreased TE. This finding is consistent with previous literature that ribosome biogenesis is downregulated during differentiation[24,25,83] and suggests that ribosome biogenesis is regulated at the level of translation. At late stages of differentiation, the transcriptome showed an upregulation of genes enriched in polar granules. This was not reflected in the Ribo-seq, likely because many of these genes were shown to be translationally repressed at the early stages of oogenesis[54].

At both the level of transcription and translation, we observed two distinct waves of gene expression changes: at 5-9 hr and 28-38 hr AHS there were many changes relative to 'no HS', while 18 hr AHS is most similar to the 'no HS' undifferentiated sample, indicating an inflection point. Interestingly, the genes changing in each wave had minimal overlap, suggesting that differentiation to a new fate involves two separate phases rather than by the gradual accumulation of changes. The inflection point at 18 hr AHS shows surprisingly few differences to the GSC-like 'no HS' sample, but has a very different forward trajectory of gene expression changes. The first wave is driven by the introduction of Bam protein via the heat shock, and Bam levels have resolved near to background levels by 18 hr AHS. However, the cells at 18 hr AHS do not return to a stable GSC-like fate, and instead embark on the second phase of differentiation without further extrinsic stimulus. We hypothesise that changes inherited through the first phase are responsible for directing this intermediate stage into the second phase of differentiation. Additional changes may persist at the protein level, but directly comparing expression between 18 hr AHS and the 'no HS' sample, two changes stand out: the loss of *bgcn* mRNA and the change in *Rbfox1* splicing to produce the cytoplasmic isoform. Bgcn acts with Bam to antagonise the action of Pum, a translational repressor which blocks differentiation of the GSC[15,84]. At 18 hr AHS neither Bam nor Bgcn is present, but the alternatively spliced cytoplasmic Rbfox1 isoform has emerged. Rbfox1 is thought to control the transition from the mitotic to post-mitotic stages of differentiation[16] and prevent the reversion into a stem cell fate by repressing translation of *pum*[17]. We speculate that a second pulse of Bam at 18 hr AHS would lead to a very different regulatory trajectory, due to the loss of Bgcn and presence of cytoplasmic Rbfox1.

We analysed how mRNA level and translation efficiency each contribute to changes in translation during differentiation. Changing both the mRNA level and translation efficiency in the same direction has an amplifying effect, but this 'intensified' category made up a minority of regulatory events, perhaps because multiple regulatory mechanisms would be superfluous. Indeed, when both mRNA level and translation efficiency acted on the same gene, they most frequently acted in the opposite direction (buffering the level of translation). The buffered category includes genes which are upregulated at the mRNA level but remain translationally repressed, enabling a preparatory transformation of the transcriptome without immediately affecting the protein complement of the cell. Indeed, we found that many of these genes are translated later in oogenesis or embryonic development. Alternatively, in some cases buffering may be a mechanism of modulating the translation efficiency to enact a more precise regulation than by changing mRNA level alone.

Altogether, we have uncovered two phases of gene expression change, which may first drive mitosis and the removal of the self-renewal fate, and subsequently promote terminal differentiation. Many adult stem cells undergo a transit amplifying stage to increase cell number before terminal differentiation. Therefore, the gene regulatory mechanisms uncovered here may be broadly applicable to these stem cell systems, including in the larval brain as well as intestine, skin and hematopoietic systems[2–6]. Furthermore, the datasets presented here can also be interrogated at a single pathway or gene level to provide insight into a large diversity of biological questions during differentiation. In this way, it will be a valuable resource for stem cell and developmental biologists.

Acknowledgments
We thank Ruth Lehmann for reagents and antibodies; Juan Mata and Caia Duncan for technical assistance with Ribo-seq experiments; the Vienna Drosophila Resource Center, and the Bloomington Drosophila Stock Center for fly reagents; AD Hay and KZA Grobicki for comments on the manuscript. TJS is a Herchel Smith Postdoctoral Fellow and DG is supported by a Walter Benjamin Postdoctoral Fellowship from Deutsche Forschungsgemeinschaft (GE3407/1-1). FKT is a Wellcome Trust and Royal Society Sir Henry Dale Fellow (206257/Z/17/Z) and is supported by the Human Frontier Science Program (CDA-00032/2018). For the purpose of Open Access, the author has applied a CC BY public copyright licence to any Author Accepted Manuscript (AAM) version arising from this submission.

Author contributions
TJS, JG and FKT conceived the idea and designed the experiments. TJS and JG performed the experiments. TJS, DG and FKT analysed the sequencing data. TJS and FKT wrote the manuscript.

Declaration of Interests
Authors declare no competing interests.

References
1. Morrison, S.J., and Spradling, A.C. (2008). Stem Cells and Niches: Mechanisms That Promote Stem Cell Maintenance throughout Life. Cell *132*, 598–611. 10.1016/j.cell.2008.01.038.

2. Homem, C.C.F., and Knoblich, J.A. (2012). Drosophila neuroblasts: A model for stem cell biology. Development (Cambridge) *139*, 4297–4310. 10.1242/dev.080515.

3. Watt, F.M. (2001). Stem cell fate and patterning in mammalian epidermis. Current Opinion in Genetics & Development *11*, 410–417. 10.1016/S0959-437X(00)00211-2.

4. Micchelli, C.A., and Perrimon, N. (2006). Evidence that stem cells reside in the adult Drosophila midgut epithelium. Nature *439*, 475–479. 10.1038/nature04371.

5. Blanpain, C., and Fuchs, E. (2006). Epidermal Stem Cells of the Skin. Annu. Rev. Cell Dev. Biol. *22*, 339–373. 10.1146/annurev.cellbio.22.010305.104357.

6. Comazzetto, S., Shen, B., and Morrison, S.J. (2021). Niches that regulate stem cells and hematopoiesis in adult bone marrow. Developmental Cell *56*, 1848–1860. 10.1016/j.devcel.2021.05.018.

7. Spradling, A., Fuller, M.T., Braun, R.E., and Yoshida, S. (2011). Germline stem cells. Cold Spring Harbor Perspectives in Biology *3*. 10.1101/cshperspect.a002642.

8. Xie, T., and Spradling, A.C. (2000). A Niche Maintaining Germ Line Stem Cells in the *Drosophila* Ovary. Science *290*, 328–330. 10.1126/science.290.5490.328.

9. McKearin, D.M., and Spradling, A.C. (1990). bag-of-marbles: a Drosophila gene required to initiate both male and female gametogenesis. Genes & Development *4*, 2242–2251. 10.1101/gad.4.12b.2242.

10. Chen, D., and McKearin, D.M. (2003). A discrete transcriptional silencer in the bam gene determines asymmetric division of the Drosophila germline stem cell. Development *130*, 1159–1170. 10.1242/dev.00325.

11. Chen, D., and McKearin, D. (2003). Dpp Signaling Silences bam Transcription Directly to Establish Asymmetric Divisions of Germline Stem Cells. Current Biology *13*, 1786–1791. 10.1016/j.cub.2003.09.033.

12. Slaidina, M., and Lehmann, R. (2014). Translational control in germline stem cell development. Journal of Cell Biology *207*, 13–21. 10.1083/jcb.201407102.

13. Forbes, A., and Lehmann, R. (1998). Nanos and Pumilio have critical roles in the development and function of *Drosophila* germline stem cells. Development *125*, 679–690. 10.1242/dev.125.4.679.

14. Wang, Z., and Lin, H. (2004). *Nanos* Maintains Germline Stem Cell Self-Renewal by Preventing Differentiation. Science *303*, 2016–2019. 10.1126/science.1093983.

15. Li, Y., Minor, N.T., Park, J.K., McKearin, D.M., and Maines, J.Z. (2009). Bam and Bgcn antagonize *Nanos* -dependent germ-line stem cell maintenance.

Proc. Natl. Acad. Sci. U.S.A. *106*, 9304–9309. 10.1073/pnas.0901452106.

16. Tastan, Ö.Y., Maines, J.Z., Li, Y., Mckearin, D.M., and Buszczak, M. (2010). *Drosophila* Ataxin 2-binding protein 1 marks an intermediate step in the molecular differentiation of female germline cysts. Development *137*, 3167–3176. 10.1242/dev.050575.

17. Carreira-Rosario, A., Bhargava, V., Hillebrand, J., Kollipara, R.K., Ramaswami, M., and Buszczak, M. (2016). Repression of Pumilio Protein Expression by Rbfox1 Promotes Germ Cell Differentiation. Developmental Cell *36*, 562–571. 10.1016/j.devcel.2016.02.010.

18. Richter, J.D., and Lasko, P. (2011). Translational Control in Oocyte Development. Cold Spring Harbor Perspectives in Biology *3*, a002758–a002758. 10.1101/cshperspect.a002758.

19. Sanchez, C.G., Teixeira, F.K., Czech, B., Preall, J.B., Zamparini, A.L., Seifert, J.R.K., Malone, C.D., Hannon, G.J., and Lehmann, R. (2016). Regulation of Ribosome Biogenesis and Protein Synthesis Controls Germline Stem Cell Differentiation. Cell Stem Cell *18*, 276–290. 10.1016/j.stem.2015.11.004.

20. Mathieu, J., Cauvin, C., Moch, C., Radford, S.J., Sampaio, P., Perdigoto, C.N., Schweisguth, F., Bardin, A.J., Sunkel, C.E., McKim, K., et al. (2013). Aurora B and Cyclin B Have Opposite Effects on the Timing of Cytokinesis Abscission in Drosophila Germ Cells and in Vertebrate Somatic Cells. Developmental Cell *26*, 250–265. 10.1016/j.devcel.2013.07.005.

21. Matias, N.R., Mathieu, J., and Huynh, J.-R. (2015). Abscission Is Regulated by the ESCRT-III Protein Shrub in Drosophila Germline Stem Cells. PLoS Genet *11*, e1004653. 10.1371/journal.pgen.1004653.

22. Eikenes, Å.H., Malerød, L., Christensen, A.L., Steen, C.B., Mathieu, J., Nezis, I.P., Liestøl, K., Huynh, J.-R., Stenmark, H., and Haglund, K. (2015). ALIX and ESCRT-III Coordinately Control Cytokinetic Abscission during Germline Stem Cell Division In Vivo. PLoS Genet *11*, e1004904. 10.1371/journal.pgen.1004904.

23. Mathieu, J., Michel-Hissier, P., Boucherit, V., and Huynh, J.-R. (2022). The deubiquitinase USP8 targets ESCRT-III to promote incomplete cell division. Science *376*, 818–823. 10.1126/science.abg2653.

24. Neumüller, R.A., Betschinger, J., Fischer, A., Bushati, N., Poernbacher, I., Mechtler, K., Cohen, S.M., and Knoblich, J.A. (2008). Mei-P26 regulates microRNAs and cell growth in the Drosophila ovarian stem cell lineage. Nature *454*, 241–245. 10.1038/nature07014.

25. Zhang, Q., Shalaby, N.A., and Buszczak, M. (2014). Changes in rRNA Transcription Influence Proliferation and Cell Fate Within a Stem Cell Lineage. Science *343*.

26. Gui, J., Samuels, T.J., Grobicki, K.Z.A., and Teixeira, F.K. (2023). Simultaneous activation of Tor and suppression of ribosome biogenesis by TRIM-NHL proteins promotes terminal differentiation. Cell Reports *42*, 112181. 10.1016/j.celrep.2023.112181.

27. Grieder, N.C., Cuevas, M. de, and Spradling, A.C. (2000). The fusome organizes the microtubule network during oocyte differentiation in *Drosophila*. Development *127*, 4253–4264. 10.1242/dev.127.19.4253.

28. Ephrussi, A., Dickinson, L.K., and Lehmann, R. (1991). oskar organizes the germ plasm and directs localization of the posterior determinant nanos. Cell *66*, 37–50. 10.1016/0092-8674(91)90137-N.

29. Lantz, V., Chang, J.S., Horabin, J.I., Bopp, D., and Schedl, P. (1994). The Drosophila orb RNA-binding protein is required for the formation of the egg chamber and establishment of polarity. Genes Dev. *8*, 598–613. 10.1101/gad.8.5.598.

30. Cox, R.T., and Spradling, A.C. (2003). A Balbiani body and the fusome mediate mitochondrial inheritance during *Drosophila* oogenesis. Development *130*, 1579–1590. 10.1242/dev.00365.

31. Teixeira, F.K., Sanchez, C.G., Hurd, T.R., Seifert, J.R.K., Czech, B., Preall, J.B., Hannon, G.J., and Lehmann, R. (2015). ATP synthase promotes germ cell differentiation independent of oxidative phosphorylation. Nat Cell Biol *17*, 689–696. 10.1038/ncb3165.

32. Christophorou, N., Rubin, T., and Huynh, J.-R. (2013). Synaptonemal Complex Components Promote Centromere Pairing in Pre-meiotic Germ Cells. PLoS Genet *9*, e1004012. 10.1371/journal.pgen.1004012.

33. Jambor, H., Surendranath, V., Kalinka, A.T., Mejstrik, P., Saalfeld, S., and Tomancak, P. (2015). Systematic imaging reveals features and changing localization of mRNAs in Drosophila development. eLife *4*, e05003. 10.7554/eLife.05003.

34. Kai, T., Williams, D., and Spradling, A.C. (2005). The expression profile of purified Drosophila germline stem cells. Developmental Biology *283*, 486–502. 10.1016/j.ydbio.2005.04.018.

35. DeLuca, S.Z., Ghildiyal, M., Pang, L.-Y., and Spradling, A.C. (2020). Differentiating Drosophila female germ cells initiate Polycomb silencing by regulating PRC2-interacting proteins. eLife *9*, e56922. 10.7554/eLife.56922.

36. Blatt, P., Wong-Deyrup, S.W., McCarthy, A., Breznak, S., Hurton, M.D., Upadhyay, M., Bennink, B., Camacho, J., Lee, M.T., and Rangan, P. (2021). RNA degradation is required for the germ-cell to maternal transition in Drosophila. Current Biology *31*, 2984-2994.e7. 10.1016/j.cub.2021.04.052.

37. Pang, L.-Y., DeLuca, S., Zhu, H., Urban, J.M., and Spradling, A.C. (2023). Chromatin and gene expression changes during female Drosophila germline stem cell development illuminate the biology of highly potent stem cells. eLife *12*, RP90509. 10.7554/eLife.90509.2.

38. Jevitt, A., Chatterjee, D., Xie, G., Wang, X.-F., Otwell, T., Huang, Y.-C., and Deng, W.-M. (2020). A single-cell atlas of adult Drosophila ovary identifies transcriptional programs and somatic cell lineage regulating oogenesis. PLoS Biol *18*, e3000538. 10.1371/journal.pbio.3000538.

39. Rust, K., Byrnes, L.E., Yu, K.S., Park, J.S., Sneddon, J.B., Tward, A.D., and Nystul, T.G. (2020). A single-cell atlas and lineage analysis of the adult Drosophila ovary. Nat Commun *11*, 5628. 10.1038/s41467-020-19361-0.

40. Slaidina, M., Gupta, S., Banisch, T.U., and Lehmann, R. (2021). A single-cell atlas reveals unanticipated cell type complexity in *Drosophila* ovaries. Genome Res. *31*, 1938–1951. 10.1101/gr.274340.120.

41. Sun, Z., Nystul, T.G., and Zhong, G. (2022). Single-cell RNA sequencing identifies regulators of differentiation and nutritional cues in *Drosophila* female germ cells (Genetics) 10.1101/2022.08.15.504025.

42. VanInsberghe, M., Van Den Berg, J., Andersson-Rolf, A., Clevers, H., and Van Oudenaarden, A. (2021). Single-cell Ribo-seq reveals cell cycle-dependent translational pausing. Nature *597*, 561–565. 10.1038/s41586-021-03887-4.

43. Ohlstein, B., and McKearin, D. (1997). Ectopic expression of the *Drosophila* Bam protein eliminates oogenic germline stem cells. Development *124*, 3651–3662. 10.1242/dev.124.18.3651.

44. Kim, J., Lu, C., Srinivasan, S., Awe, S., Brehm, A., and Fuller, M.T. (2017). Blocking promiscuous activation at cryptic promoters directs cell type–specific gene expression. Science *356*, 717–721. 10.1126/science.aal3096.

45. Lu, D., Sin, H.-S., Lu, C., and Fuller, M.T. (2020). Developmental regulation of cell type-specific transcription by novel promoter-proximal sequence elements. Genes Dev. *34*, 663–677. 10.1101/gad.335331.119.

46. Wilcockson, S.G., and Ashe, H.L. (2019). Drosophila Ovarian Germline Stem Cell Cytocensor Projections Dynamically Receive and Attenuate BMP Signaling. Developmental Cell *50*, 296-312.e5. 10.1016/j.devcel.2019.05.020.

47. McCarthy, A., Sarkar, K., Martin, E.T., Upadhyay, M., Jang, S., Williams, N.D., Forni, P.E., Buszczak, M., and Rangan, P. (2022). Msl3 promotes germline stem cell differentiation in female *Drosophila*. Development *149*, dev199625. 10.1242/dev.199625.

48. Kai, T., and Spradling, A. (2004). Differentiating germ cells can revert into functional stem cells in Drosophila melanogaster ovaries. Nature *428*, 564–569. 10.1038/nature02436.

49. Lin, H., Yue, L., and Spradling, A.C. (1994). The *Drosophila* fusome, a germline-specific organelle,

contains membrane skeletal proteins and functions in cyst formation. Development *120*, 947–956. 10.1242/dev.120.4.947.

50. Cuevas, M. de, and Spradling, A.C. (1998). Morphogenesis of the *Drosophila* fusome and its implications for oocyte specification. Development *125*, 2781–2789. 10.1242/dev.125.15.2781.

51. McKearin, D., and Ohlstein, B. (1995). A role for the Drosophila Bag-of-marbles protein in the differentiation of cystoblasts from germline stem cells. Development *121*, 2937–2947.

52. Ohlstein, B., Lavoie, C.A., Vef, O., Gateff, E., and McKearin, D.M. (2000). The Drosophila Cystoblast Differentiation Factor, *benign gonial cell neoplasm* , Is Related to DExH-box Proteins and Interacts Genetically With *bag-of-marbles*. Genetics *155*, 1809–1819. 10.1093/genetics/155.4.1809.

53. Pauli, D., Arrigo, A.-P., and Tissières, A. (1992). Heat shock response inDrosophila. Experientia *48*, 623–629. 10.1007/BF02118306.

54. Lehmann, R. (2016). Germ Plasm Biogenesis—An Oskar-Centric Perspective. In Current Topics in Developmental Biology (Elsevier), pp. 679–707. 10.1016/bs.ctdb.2015.11.024.

55. Wang, Q., and Rio, D.C. (2018). JUM is a computational method for comprehensive annotation-free analysis of alternative pre-mRNA splicing patterns. Proc. Natl. Acad. Sci. U.S.A. *115*. 10.1073/pnas.1806018115.

56. Yue, L., and Spradling, A.C. (1992). hu-li tai shao, a gene required for ring canal formation during Drosophila oogenesis, encodes a homolog of adducin. Genes & Development *6*, 2443–2454. 10.1101/gad.6.12b.2443.

57. Whittaker, K.L., Ding, D., Fisher, W.W., and Lipshitz, H.D. (1999). Different 3′ untranslated regions target alternatively processed *hu-li tai shao* (*hts*) transcripts to distinct cytoplasmic locations during *Drosophila* oogenesis. Journal of Cell Science *112*, 3385–3398. 10.1242/jcs.112.19.3385.

58. Gerdes, J.A., Mannix, K.M., Hudson, A.M., and Cooley, L. (2020). HtsRC-Mediated Accumulation of F-Actin Regulates Ring Canal Size During *Drosophila melanogaster* Oogenesis. Genetics *216*, 717–734. 10.1534/genetics.120.303629.

59. Sugimura, I., and Lilly, M.A. (2006). Bruno Inhibits the Expression of Mitotic Cyclins during the Prophase I Meiotic Arrest of Drosophila Oocytes. Developmental Cell *10*, 127–135. 10.1016/j.devcel.2005.10.018.

60. Kim-Ha, J., Kim, J., and Kim, Y.-J. (1999). Requirement of RBP9, a *Drosophila* Hu Homolog, for Regulation of Cystocyte Differentiation and Oocyte Determination during Oogenesis. Molecular and Cellular Biology *19*, 2505–2514. 10.1128/MCB.19.4.2505.

61. Morris, S.A. (2019). The evolving concept of cell identity in the single cell era. Development *146*, dev169748. 10.1242/dev.169748.

62. Brunet Avalos, C., Maier, G.L., Bruggmann, R., and Sprecher, S.G. (2019). Single cell transcriptome atlas of the Drosophila larval brain. eLife *8*, e50354. 10.7554/eLife.50354.

63. Schiebinger, G., Shu, J., Tabaka, M., Cleary, B., Subramanian, V., Solomon, A., Gould, J., Liu, S., Lin, S., Berube, P., et al. (2019). Optimal-Transport Analysis of Single-Cell Gene Expression Identifies Developmental Trajectories in Reprogramming. Cell *176*, 928-943.e22. 10.1016/j.cell.2019.01.006.

64. Farrell, J.A., Wang, Y., Riesenfeld, S.J., Shekhar, K., Regev, A., and Schier, A.F. (2018). Single-cell reconstruction of developmental trajectories during zebrafish embryogenesis. Science *360*, eaar3131. 10.1126/science.aar3131.

65. Vogel, C., and Marcotte, E.M. (2012). Insights into the regulation of protein abundance from proteomic and transcriptomic analyses. Nat Rev Genet *13*, 227–232. 10.1038/nrg3185.

66. Aspden, J.L., Eyre-Walker, Y.C., Phillips, R.J., Amin, U., Mumtaz, M.A.S., Brocard, M., and Couso, J.-P. (2014). Extensive translation of small Open Reading Frames revealed by Poly-Ribo-Seq. eLife *3*, e03528. 10.7554/eLife.03528.

67. Douka, K., Agapiou, M., Birds, I., and Aspden, J.L. (2022). Optimization of Ribosome Footprinting Conditions for Ribo-Seq in Human and Drosophila

melanogaster Tissue Culture Cells. Front. Mol. Biosci. *8*, 791455. 10.3389/fmolb.2021.791455.

68. Dunn, J.G., Foo, C.K., Belletier, N.G., Gavis, E.R., and Weissman, J.S. (2013). Ribosome profiling reveals pervasive and regulated stop codon readthrough in Drosophila melanogaster. eLife *2*, e01179. 10.7554/eLife.01179.

69. Kronja, I., Yuan, B., Eichhorn, S.W., Dzeyk, K., Krijgsveld, J., Bartel, D.P., and Orr-Weaver, T.L. (2014). Widespread Changes in the Posttranscriptional Landscape at the Drosophila Oocyte-to-Embryo Transition. Cell Reports *7*, 1495–1508. 10.1016/j.celrep.2014.05.002.

70. Jang, S., Lee, J., Mathews, J., Ruess, H., Williford, A.O., Rangan, P., Betrán, E., and Buszczak, M. (2021). The *Drosophila* ribosome protein S5 paralog RpS5b promotes germ cell and follicle cell differentiation during oogenesis. Development *148*, dev199511. 10.1242/dev.199511.

71. Kim-Ha, J., Smith, J.L., and Macdonald, P.M. (1991). oskar mRNA is localized to the posterior pole of the Drosophila oocyte. Cell *66*, 23–35. 10.1016/0092-8674(91)90136-M.

72. Kim-Ha, J., Kerr, K., and Macdonald, P.M. (1995). Translational regulation of oskar mRNA by Bruno, an ovarian RNA-binding protein, is essential. Cell *81*, 403–412. 10.1016/0092-8674(95)90393-3.

73. Sarov, M., Barz, C., Jambor, H., Hein, M.Y., Schmied, C., Suchold, D., Stender, B., Janosch, S., Kj, V.V., Krishnan, R., et al. (2016). A genome-wide resource for the analysis of protein localisation in Drosophila. eLife *5*, e12068. 10.7554/eLife.12068.

74. Greenblatt, E.J., and Spradling, A.C. (2018). Fragile X mental retardation 1 gene enhances the translation of large autism-related proteins. Science *361*, 709–712. 10.1126/science.aas9963.

75. DiMario, P.J., and Mahowald, A.P. (1987). Female sterile (1) yolkless: a recessive female sterile mutation in Drosophila melanogaster with depressed numbers of coated pits and coated vesicles within the developing oocytes. The Journal of cell biology *105*, 199–206. 10.1083/jcb.105.1.199.

76. Hara, M., Petrova, B., and Orr-Weaver, T.L. (2017). Control of PNG kinase, a key regulator of mRNA translation, is coupled to meiosis completion at egg activation. eLife *6*, e22219. 10.7554/eLife.22219.

77. Tadros, W., Goldman, A.L., Babak, T., Menzies, F., Vardy, L., Orr-Weaver, T., Hughes, T.R., Westwood, J.T., Smibert, C.A., and Lipshitz, H.D. (2007). SMAUG Is a Major Regulator of Maternal mRNA Destabilization in Drosophila and Its Translation Is Activated by the PAN GU Kinase. Developmental Cell *12*, 143–155. 10.1016/j.devcel.2006.10.005.

78. Manheim, E.A., Jang, J.K., Dominic, D., and McKim, K.S. (2002). Cytoplasmic Localization and Evolutionary Conservation of MEI-218, a Protein Required for Meiotic Crossing-over in *Drosophila*. MBoC *13*, 84–95. 10.1091/mbc.01-06-0318.

79. Chothani, S., Adami, E., Ouyang, J.F., Viswanathan, S., Hubner, N., Cook, S.A., Schafer, S., and Rackham, O.J.L. (2019). deltaTE: Detection of Translationally Regulated Genes by Integrative Analysis of Ribo-seq and RNA-seq Data. Current Protocols in Molecular Biology *129*. 10.1002/cpmb.108.

80. Teixeira, F.K., and Lehmann, R. (2019). Translational Control during Developmental Transitions. Cold Spring Harb Perspect Biol *11*, a032987. 10.1101/cshperspect.a032987.

81. Parisi, M.J., Deng, W., Wang, Z., and Lin, H. (2001). Thearrest gene is required for germline cyst formation duringDrosophila oogenesis. genesis *29*, 196–209. 10.1002/gene.1024.

82. Wang, Z., and Lin, H. (2007). Sex-lethal is a target of Bruno-mediated translational repression in promoting the differentiation of stem cell progeny during Drosophila oogenesis. Developmental Biology *302*, 160–168. 10.1016/j.ydbio.2006.09.016.

83. Martin, E.T., Blatt, P., Nguyen, E., Lahr, R., Selvam, S., Yoon, H.A.M., Pocchiari, T., Emtenani, S., Siekhaus, D.E., Berman, A., et al. (2022). A translation control module coordinates germline stem cell differentiation with ribosome biogenesis during Drosophila oogenesis. Developmental Cell *57*, 883-900.e10. 10.1016/j.devcel.2022.03.005.

84. Kim, J.Y., Lee, Y.C., and Kim, C. (2010). Direct Inhibition of Pumilo Activity by Bam and Bgcn in Drosophila Germ Line Stem Cell Differentiation. Journal of Biological Chemistry *285*, 4741–4746. 10.1074/jbc.M109.002014.

85. Gaspar, I., Wippich, F., and Ephrussi, A. (2017). Enzymatic production of single-molecule FISH and RNA capture probes. RNA *23*, 1582–1591. 10.1261/rna.061184.117.

86. Schindelin, J., Arganda-Carreras, I., Frise, E., Kaynig, V., Longair, M., Pietzsch, T., Preibisch, S., Rueden, C., Saalfeld, S., Schmid, B., et al. (2012). Fiji: an open-source platform for biological-image analysis. Nat Methods *9*, 676–682. 10.1038/nmeth.2019.

87. Morlan, J.D., Qu, K., and Sinicropi, D.V. (2012). Selective Depletion of rRNA Enables Whole Transcriptome Profiling of Archival Fixed Tissue. PLoS ONE *7*, e42882. 10.1371/journal.pone.0042882.

88. ElMaghraby, M.F., Andersen, P.R., Pühringer, F., Hohmann, U., Meixner, K., Lendl, T., Tirian, L., and Brennecke, J. (2019). A Heterochromatin-Specific RNA Export Pathway Facilitates piRNA Production. Cell *178*, 964-979.e20. 10.1016/j.cell.2019.07.007.

89. Martin, M. (2011). Cutadapt removes adapter sequences from high-throughput sequencing reads. EMBnet j. *17*, 10. 10.14806/ej.17.1.200.

90. Langmead, B., Trapnell, C., Pop, M., and Salzberg, S.L. (2009). Ultrafast and memory-efficient alignment of short DNA sequences to the human genome. 10.13016/KIY1-GYZY.

91. Langmead, B., and Salzberg, S.L. (2012). Fast gapped-read alignment with Bowtie 2. Nature Methods *9*, 357–359. 10.1038/nmeth.1923.

92. Dobin, A., Davis, C.A., Schlesinger, F., Drenkow, J., Zaleski, C., Jha, S., Batut, P., Chaisson, M., and Gingeras, T.R. (2013). STAR: Ultrafast universal RNA-seq aligner. Bioinformatics *29*, 15–21. 10.1093/bioinformatics/bts635.

93. Trapnell, C., Williams, B.A., Pertea, G., Mortazavi, A., Kwan, G., Van Baren, M.J., Salzberg, S.L., Wold, B.J., and Pachter, L. (2010). Transcript assembly and quantification by RNA-Seq reveals unannotated transcripts and isoform switching during cell differentiation. Nature Biotechnology *28*, 511–515. 10.1038/nbt.1621.

94. Liao, Y., Smyth, G.K., and Shi, W. (2014). featureCounts: an efficient general purpose program for assigning sequence reads to genomic features. Bioinformatics *30*, 923–930. 10.1093/bioinformatics/btt656.

95. Lyne, R., Smith, R., Rutherford, K., Wakeling, M., Varley, A., Guillier, F., Janssens, H., Ji, W., Mclaren, P., North, P., et al. (2007). FlyMine: an integrated database for Drosophila and Anopheles genomics. Genome Biol *8*, R129. 10.1186/gb-2007-8-7-r129.

Materials and Methods

Resource availability

Lead Contact

Further information and requests for resources or reagents should be directed to the lead contact Felipe Karam Teixeira (fk319@cam.ac.uk).

Data and code availability

RNA-seq and Ribo-seq data generated during this current study will be deposited at GEO and will be publicly available as of the date of publication. This paper does not report original code. Any additional information required to reanalyse the data reported in this paper is available from the lead contact upon request.

Drosophila husbandry and genetics

Unless otherwise stated, stocks and crosses were maintained on standard propionic food at 25°C for experiments. The *Drosophila melanogaster* stocks used were:

***Drosophila* stock**	**genotype**	**Origin**
wild type	*w[1118]*	R. Lehmann lab
bam mutant	*ry[506] e[1] bam[Δ86]/TM3, ry[RK] Sb[1] Ser[1]*	BDSC#5427
bam$^{-/-}$*,hs-bam*	*w[1118]; nosP-GAL4-NGT40/CyO; bamΔ86, P{w[+mC]=hs-bam.O}11d/TM6B*	hs-bam construct from D. McKearin
Mod FlyFOS	*PBac{fTRG00197.sfGFP-TVPTBF}VK00033*	VDRC v318495
Dp1 FlyFOS	*PBac{fTRG01340.sfGFP-TVPTBF}VK00033*	VDRC v318850
Cirl FlyFOS	*PBac{fTRG01155.sfGFP-TVPTBF}VK00033*	VDRC v318773

Synchronising GSC differentiation

Virgin females (*w[1118]; nosP-GAL4-NGT40/CyO; bamΔ86, P{w[+mC]=hs-bam.O}11d/TM6B*) were crossed to males (*w;; bamΔ86/Tm6C*). Female F1s (*w;nosP-GAL4-NGT40/+;bamΔ86, P{w[+mC]=hs-bam.O}11d/bamΔ86*) were collected overnight and fattened on yeast for three days. Flies were heatshocked in pre-warmed vials without yeast for 1 hour at 37°C, followed by 2 hours at 34°C. Flies were flipped to fresh vials with yeast, returned to 25°C and time after heat shock (AHS) was measured from this point.

smFISH probe labelling

smFISH probes (32 probes per gene) were designed using the Stellaris Probe Designer (Biosearch Technologies) and ordered as unlabelled DNA oligos. Labelling was done according to Gaspar et al., 2017[85]. Briefly, unlabelled ddUTP was conjugated to an ATTO dye NHS ester (ATTO565 or ATTO633, Atto-tec), then the labelled ddUTP was added to the 3' end of each probe with terminal deoxynucleotidyl transferase. Probes were purified by ethanol precipitation.

Antibody staining

Ovaries were dissected in cold PBS and fixed for 25 minutes at room temperature in 4% formaldehyde in 0.3% PBSTX (0.3% Triton-X). Ovaries were washed with 3x 15 mins in 0.3% PBSTX, then incubated in Block (0.2 µg/ul BSA in 0.3% PBSTX) for 1 hr at room temperature. Primary antibodies were added to Block at the appropriate concentration for incubation overnight at 4°C. The following day, washes and secondary antibody incubation were performed in Block, with the addition of Hoechst 33342 DNA stain (ThermoFisher Scientific) in one wash step.

Antibody	**Concentration**	**Origin**
Alpha-spectrin (mouse)	1:100	DSHB Cat#3A9(323 or M10-2)
Vasa (rabbit)	1:1000	Ruth Lehmann
Bam (mouse)	1:20	DSHB bam
Orb (mouse)	1:200	DSHB 4H8
GFP Booster ATTO 488	1:500	Chromotek (gba488-100)

smFISH

Ovaries were dissected and fixed as above for IF. After 3x washes in 0.3% PBSTX, samples were transferred to Wash buffer (2X saline sodium citrate (SSC), 10% deionised formamide in nuclease-free water) for 10 mins at room temperature. smFISH probes, primary antibodies and phalloidin (Alexa Fluor 405 or 488 Phalloidin, ThermoFisher Scientific) were diluted in Hybridisation buffer (2X SSC, 10% deionised formamide, 20mM vanadyl ribonucleoside complex, 0.1 mg/ml BSA, competitor (1:50 dilution of 5 mg/ml E.coli tRNA and 5 mg/ml salmon sperm ssDNA) in nuclease-free water). Ovaries were incubated in Hybridisation buffer at 37°C overnight (less than 16 hours). Ovaries were washed 3x 15 mins in Wash buffer, then incubated with secondary antibodies in Wash buffer for 2 hours at room temperature. Ovaries were finally washed in Wash buffer, with the addition of Hoechst in one wash step.

Imaging

Samples were mounted in VectaShield mounting media (Vector Laboratories). Images were acquired on a Leica SP8 confocal microscope with a 20x dry objective or 40x oil objective. Image processing was using Fiji[86].

Western blot

30 pairs of ovaries were collected for each sample and lysed in Laemmli buffer with B-mercaptoethanol. Ovaries were homogenised with an electric pestle then incubated at 95°C for 5 min. Samples were run on a Novex Value 4-12% Tris-Glycine Mini Protein Gel. Proteins were transferred to a PVDF membrane by wet transfer. Blots were blocked with 5% skimmed milk in TBST (TBS with 1% Tween) for 1 hr at room temperature. Primary antibody incubation was at 4°C overnight, then blots were washed and incubated with secondary antibodies in TBSTS (TBST with 0.01% SDS) for 30 mins at room temperature. Blots were imaged with a Licor Odyssey imager.

Antibody	**Concentration**	**Origin**
Vasa (rabbit)	1:5000	Ruth Lehmann

Bam (mouse)	1:500	DSHB bam

RNA-seq

Ovaries were dissected for each sample in cold Dissection buffer (PBS 1X, 0.01% Tween 20, 100 µg/ml cycloheximide) and immediately stored at -80°C after dissection. Frozen samples were homogenised in Polysome extraction buffer (50 mM Tris pH 7.5, 5 mM MgCl2, 150 mM NaCl, 0.5% Triton x-100, 1 mM DTT, 100 µg/ml cycloheximide, protease inhibitor, 25 u/ml Turbo DNAse) using an electrical pestle and then further disrupted by passing 20 times through a 26-gauge needle. The lysate was centrifuged at 20,000g for 10 min at 4°C to pellet tissue debris. Total RNA was isolated by hot phenol-chloroform extraction and quantified using Qubit RNA High Sensitivity Assay Kit (Invitrogen). 1.5 µg of total RNA was used for rRNA depletion by binding of complementary oligos and treatment with RNase H[87,88]. Libraries were generated using NEBNext®Ultra™ Directional RNA Library Prep Kit for Illumina® according to manufacturer's instructions. Libraries were multiplexed using the NEBNext® Multiplex Oligos for Illumina® and sequenced in paired-end 150 nt-long reads on an Illumina NovaSeq 6000.

Ribo-seq

250 pairs of ovaries were dissected for each sample in cold Dissection buffer (PBS 1X, 0.01% Tween 20, 100 µg/ml cycloheximide) and stored at -80°C. As for RNA-seq, frozen samples were homogenised with an electrical pestle in Polysome extraction buffer (50 mM Tris pH 7.5, 5 mM MgCl2, 150 mM NaCl, 0.5% Triton x-100, 1 mM DTT, 100 µg/ml cycloheximide, protease inhibitor, 25 u/ml Turbo DNAse), then passed 20 times through a 26-gauge needle. The lysate was centrifuged at 20,000g for 10 min at 4°C to pellet tissue debris. 100-140 µg of total RNA was used for Ribo-seq. Total RNA was treated with 1.25 units of RNase I (Ambion) per µg RNA, and the quenched with SuperaseIn (0.8 units per µg RNA). The sample was brought to 1 ml by adding Polysome extraction buffer and subjected to a 3 ml 34% sucrose cushion, by centrifugation at 70,000 rpm for 5.5 hr at 4°C. The resulting pellet was resuspended in nuclease free water with 1% SDS. RNA was extracted with hot phenol-chloroform and purified by Zymo RNA Clean & Concentrator kit. rRNA was depleted as for the RNA-seq through binding of complementary oligos[88] and treatment with RNase H[87]. Size selection was performed on a 15% Urea PAGE Gel, cutting the band corresponding to 28 to 34 bp. RNA was purified by ZYMO small-RNA PAGE recovery kit. RNA was treated with 1 ul of T4 PNK for end repair and libraries were produced with the NEBNext Small RNA Library Kit, according to manufacturer's instructions. Libraries were size selected at 148-154 nucleotides, corresponding to ligated constructs from 28 to 34 nt RNA fragments. Libraries were multiplexed using the NEBNext® Multiplex Oligos for Illumina® and sequenced in single-end 50 nt-long reads on an Illumina HiSeq 4000.

Data analysis

Trim galore, integrating the trimmer tool cutadapt[89], was used for adapter trimming and quality control of both (paired-end) RNA-seq and (single-end) Ribo-seq data. Subsequently, random 4 nucleotides (4N adapters) from both 3′- and 5′-ends, introduced during library preparation, were removed from Ribo-seq reads after excluding redundant reads. Trimmed reads were aligned to non-coding RNA reference sequences (flybase, dmel_r6.39) using Bowtie[90] for Ribo-seq and Bowtie2[91] for RNA-seq data and then non-matching reads were mapped to the *Drosophila melanogaster* reference genome dm6 using STAR[92]. For quality control and benchmarking of Ribo-seq data we used the R package ribosomeProfilingQC (Ou and Hoye, 2022). Transcript abundance was quantified and differentially expressed genes were identified using Cuffdiff v2.2.1[93]. Splicing analysis was performed with Jum (version 1.3.12)[55], after 2-pass mapping with STAR. For analysis of translation efficiency, read counts were generated using featureCounts[94]. Differences in translation efficiency and classification of gene regulation was analysed using deltaTE[79]. All analyses were performed with two samples, each with two biological replicates. For comparison to whole ovary, RNA-seq and Ribo-seq datasets from Greenblatt & Spradling, 2018[74] (NCBI BioProject PRJNA466150, three mCherry RNAi control samples) were reanalysed with cufflinks. GO analysis was performed using FlyMine[95]. PCA analysis was performed using the prcomp function in R, using scaled variables.

Supplementary Figures

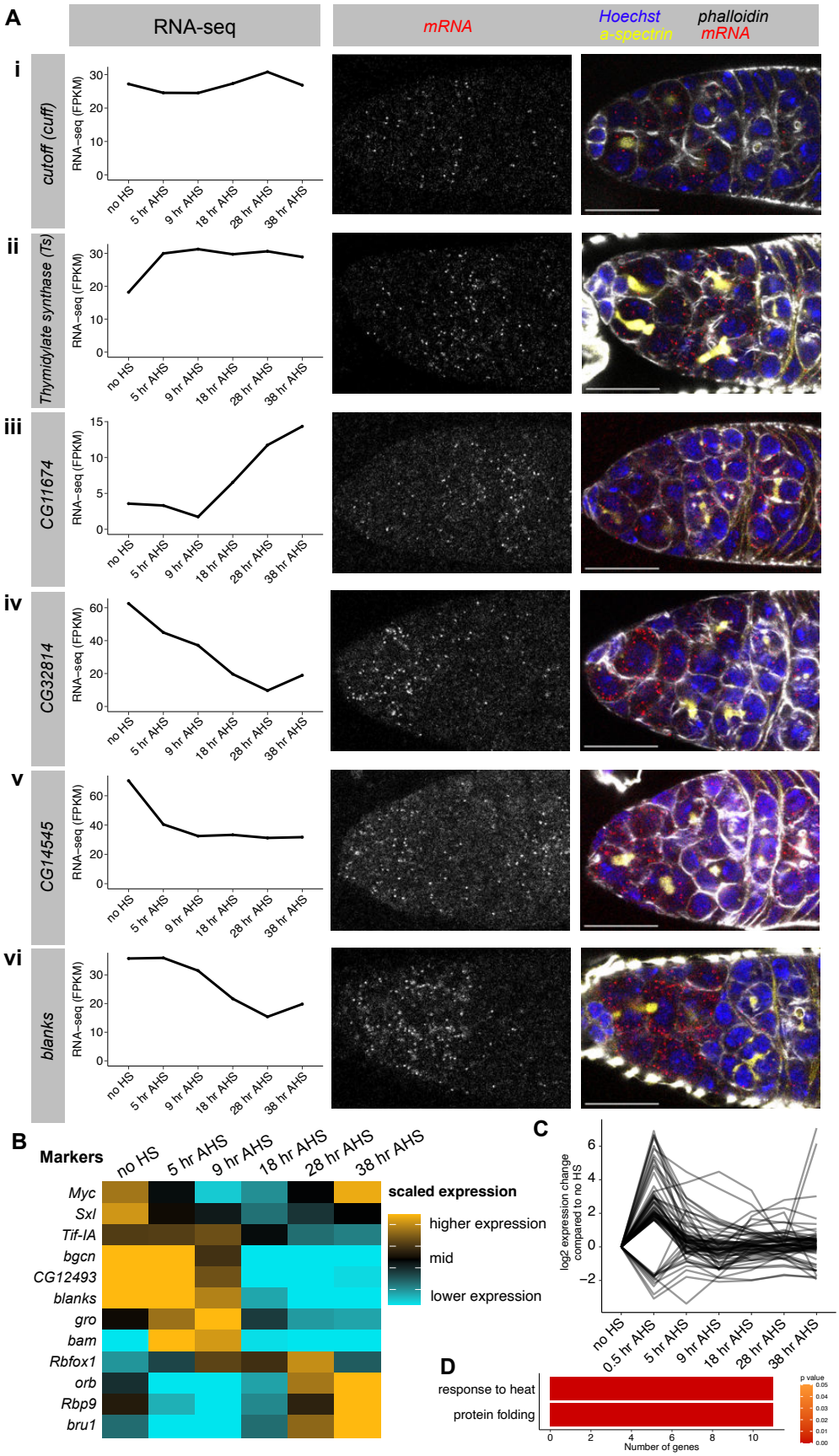

Figure S1 – RNA-seq in synchronised differentiating GSCs recapitulates changes in gene expression during normal differentiation (Related to Figure 2)

(A) As in Figure 2A, smFISH in *wild type* germaria (right) was used to validate the RNA-seq results (left). Staining for DNA (Hoechst, blue), actin (phalloidin, gray), fusome (α-spectrin, yellow), and mRNA transcript of interest (smFISH, red and grayscale): **(i)** *cuff,* **(ii)** *thymidylate synthase*, **(iii)** *CG11674,* **(iv)** *CG32814 (eggplant),* **(v)** *CG14545,* **(vi)** *blanks.* Scale bars are 15 µm. **(B)** Heatmap illustrating RNA-seq expression level across our time

course, of marker genes identified by scRNA-seq pseudotime analysis by Rust et al., 2020 (illustrated in Fig 2m in that paper) for each time point from GSC to 16cc. Each row represents one gene and expression level is scaled per gene: black - mean expression across the time course, gold - 25% higher expression than the mean, cyan - 25% lower expression than the mean. (**C**) The 0.5 hr AHS sample was used to exclude 67 genes which showed a significant change of >3-fold between the 0.5 AHS and the no HS samples (with expression >10 FPKM in one of these samples). The expression of these 67 genes is shown as log2foldchange at each time point relative to no HS. **(D)** GO analysis of the excluded 67 genes shown in **(C)** found a significant enrichment in terms associated with a heat shock response. Colour of the bar indicates p value of the enrichment.

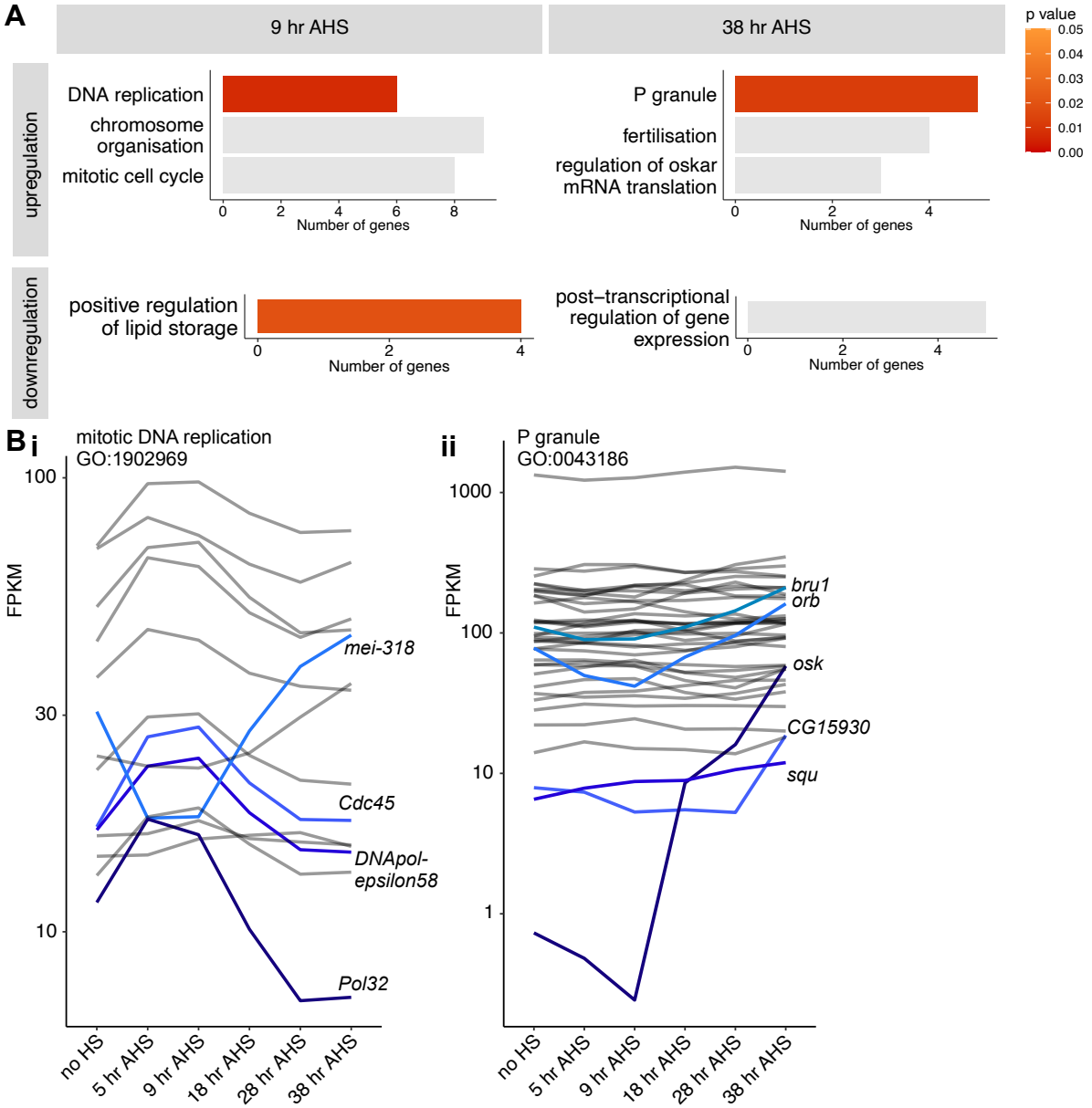

Figure S2 – RNA-seq reveals changes in mRNA level during differentiation (Related to Figure 2)
(**A**) Gene ontology analysis of genes upregulated or downregulated in the RNA-seq at 9 hr AHS or 38 hr AHS compared to 'no HS'. Colour of the bar indicates p value of the enrichment, grey = p > 0.05 (**B**) RNA-seq FPKM for genes in two gene ontology groups: mitotic DNA replication (i) and P granule (ii). Genes with a >1.6-fold change in gene expression are highlighted.

A

Time point	Replicate R^2
no HS	0.9786
0.5 hr AHS	0.9831
5 hr AHS	0.9953
9 hr AHS	0.9891
18 hr AHS	0.9948
28 hr AHS	0.9761
38 hr AHS	0.9973

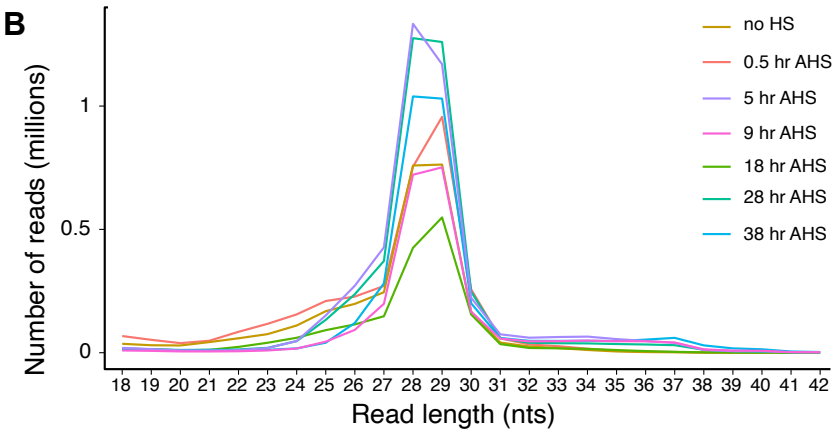

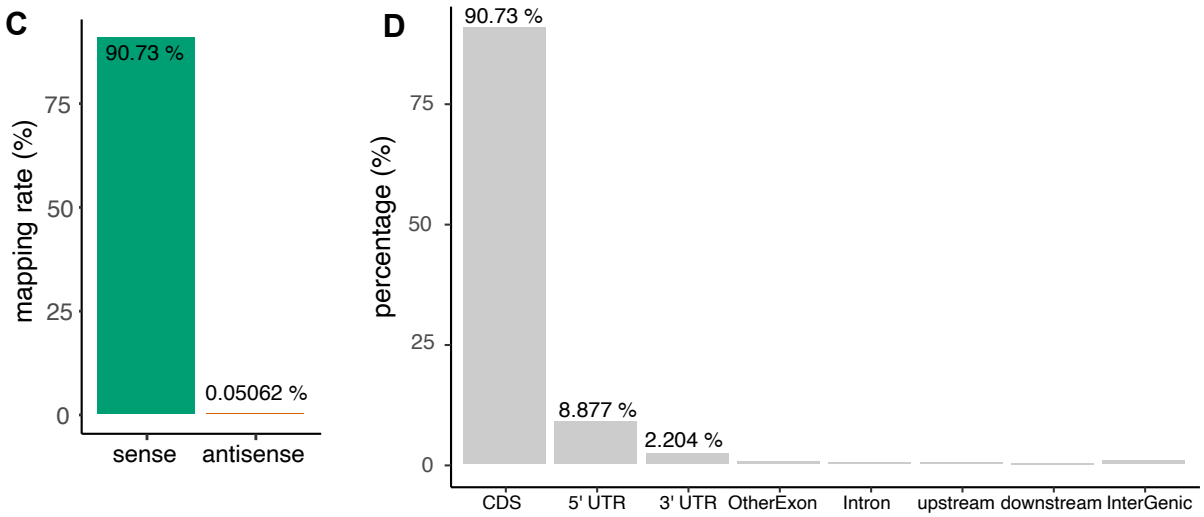

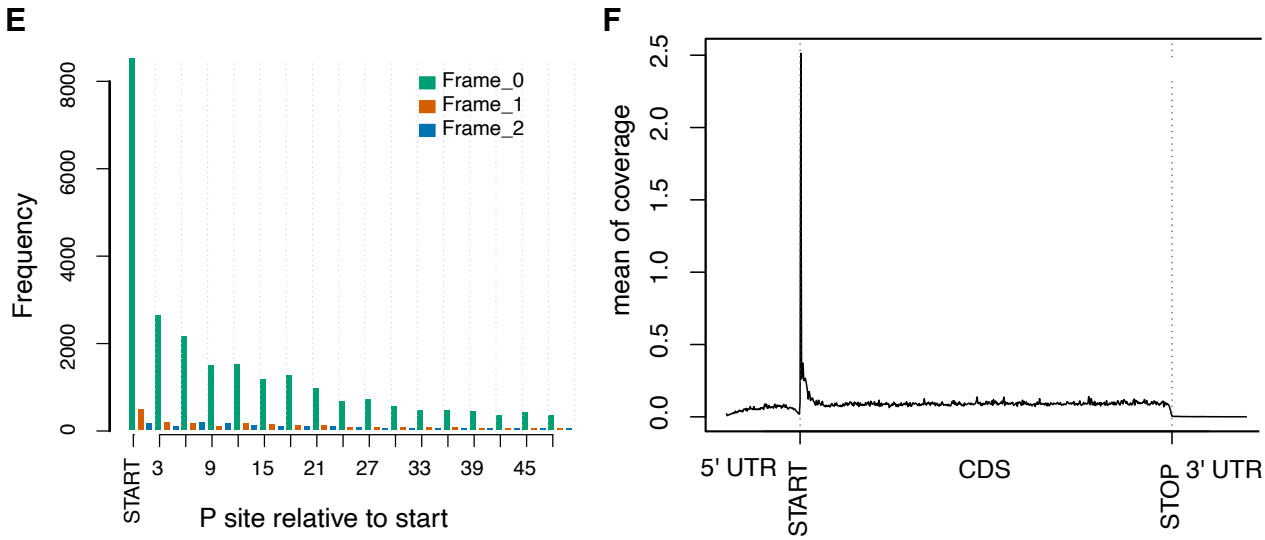

Figure S3 – Ribo-seq quality control (Related to Figure 4)

(**A**) R^2 show good correlation between Ribo-seq replicate samples at each time point. (**B**) Distribution of read length in nucleotides for Ribo-seq libraries at each time point. (**C-F**) Ribo-seq quality control for the 'no HS' sample only for illustration. (**C**) 90.73% of reads mapped to the CDS on the sense strand of genes compared to 0.05% mapping to the CDS on the antisense strand. (**D**) 8.88% of reads map to the 5' UTR, 2.20% map to the 3' UTR, and mapping to introns and intergenic regions is negligible. (**E**) P site mapping shows a strong three nucleotide periodicity, with highest frequency at the start codon. (**F**) Metagene analysis plot showing read distribution in 5' UTR, CDS and 3' UTR regions, shows consistent coverage across the CDS with the expected bias at the start codon.

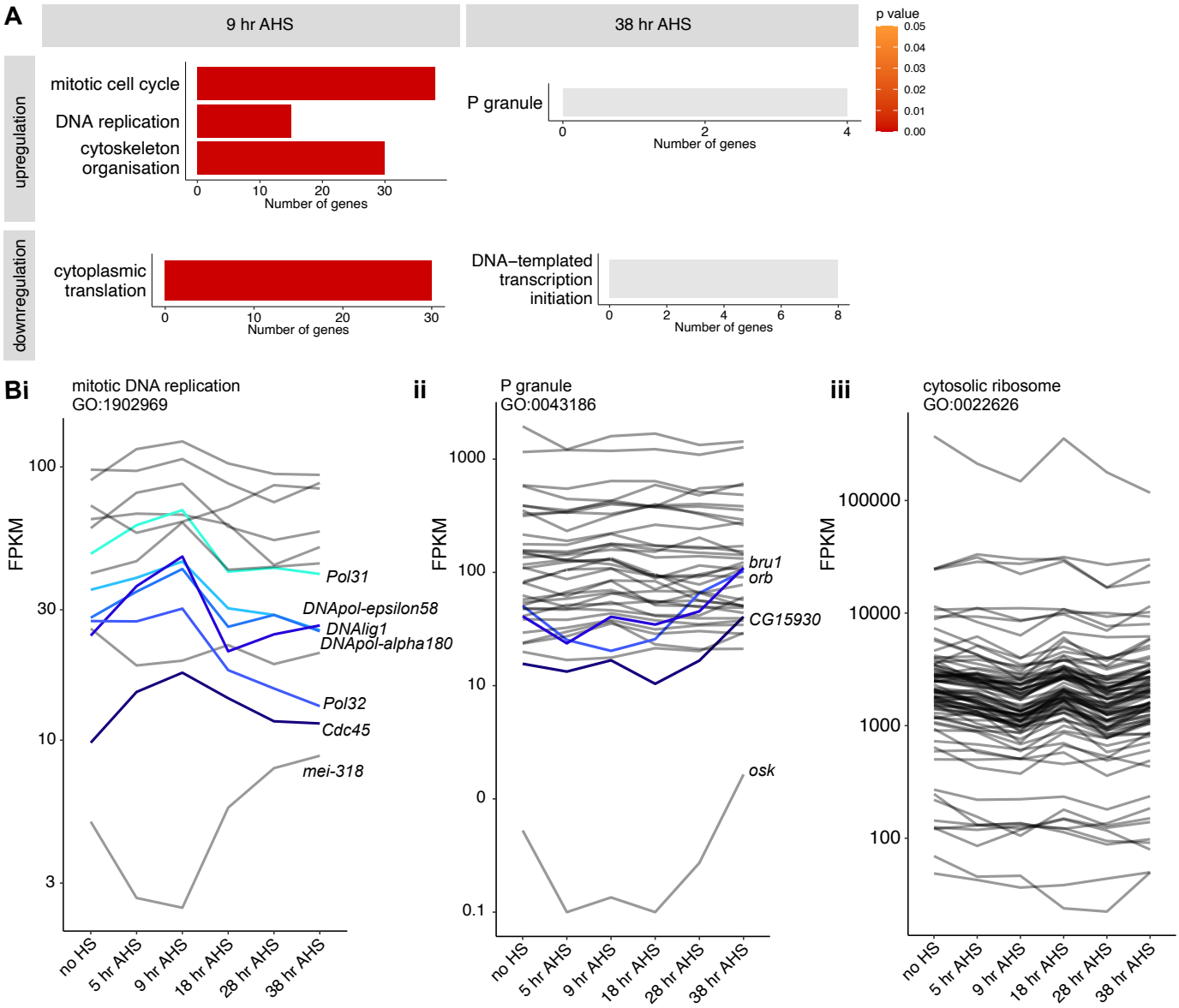

Figure S4 – Ribo-seq reveals changes in translation during GSC differentiation (Related to Figure 5)
(**A**) Gene ontology analysis of genes upregulated or downregulated in the Ribo-seq at 9 hr AHS or 38 hr AHS compared to 'no HS'. Colour of the bar indicates p value of the enrichment, grey = p > 0.05. (**B**) Ribo-seq FPKM for genes in three gene ontology groups: mitotic DNA replication (i), P granule (ii) and cytosolic ribosome (iii). Genes with a >1.6-fold change in gene expression are highlighted (except in iii due to too many genes).

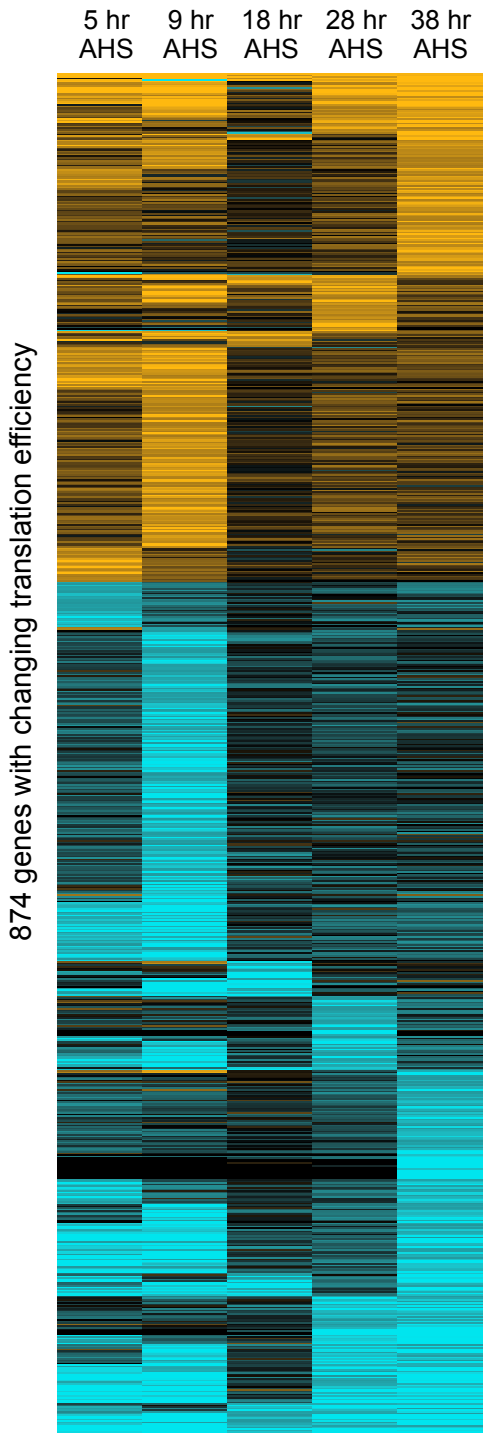

Figure S5 – Many genes are regulated by TE (Related to Figure 7)
Heat map showing fold change in TE, compared to the 'no HS' timepoint, for the 874 genes which exhibit a significant 1.6-fold change in translation between a given time point and 'no HS'. cyan = two-fold decrease compared to 'no HS', black = no change, gold = two-fold increase.

Supplementary Table 1. RNA-seq FPKMs for genes with a heat shock effect over 3-fold (significant, and over 10 FPKM), and list of contaminants.

Supplementary Table 2. rRNA depleted RNA-seq FPKMs for each time point, after filtering (>10 FPKM, removal of contaminants)

Supplementary Table 3. Ribo-seq FPKMs for each time point, for the genes as in Supplementary Table 2